AIMS Mathematics, 11(1): 2645–2681.
DOI: 10.3934/math.2026107
Received: 18 December 2025
Revised: 15 January 2026
Accepted: 23 January 2026
Published: 27 January 2026

http://www.aimspress.com/journal/Math

Research article

Modeling dual-colony Nosema transmission in honeybees: The role of distributed delays and antiviral treatment

Miled El Hajji*, Yousef A. Al-Faidi and Mohammed H. Alharbi

Department of Mathematics and Statistics, Faculty of Science, University of Jeddah, P.O. Box 80327, Jeddah 21589, Saudi Arabia

* **Correspondence:** Email: miled.elhajji@enit.rnu.tn.

Abstract: In this paper, we develop a comprehensive mathematical model to investigate the transmission dynamics of dual Nosema infections (*Nosema apis* and *Nosema ceranae*) in two interacting honeybee colonies. The model incorporates distributed time delays to capture biological realism in latency, incubation, and parasite maturation periods, and includes an environmental pathogen compartment to account for indirect, environment-mediated transmission. First, we analyze a simplified ordinary differential equation (ODE) version of the model, thereby deriving the basic reproduction number $\mathscr{R}_0$ and establishing the global asymptotic stability of both disease-free and endemic equilibria using Lyapunov functions. Then, the analysis is extended to the full distributed-delay system, where we derive the delayed basic reproduction number $\mathscr{R}_0^d$ and prove the global stability of its equilibria via carefully constructed Lyapunov functionals. A sensitivity analysis identifies key parameters—most notably transmission rates, spore shedding rates, and natural mortality—that dominate the infection dynamics. Furthermore, we introduce an antiviral treatment term to quantify the efficacy required to drive $\mathscr{R}_0^d$ below unity and achieve disease eradication. Numerical simulations validate the analytical results and illustrate how distributed delays and treatment interventions critically influence the long-term disease outcomes. The study provides a robust theoretical framework to understand Nosema spread in multi-colony settings. Its key contributions are as follows: (1) The derivation of an additive basic reproduction number reveals the necessity of apiary-wide management; (2) provides rigorous global stability proofs for the delayed system; and (3) provides actionable quantitative insights to design effective apiary management, identify critical intervention targets, and establish treatment efficacy thresholds for disease eradication.

Keywords: distributed delays; environmental transmission; basic reproduction number; global stability; Lyapunov functionals; sensitivity analysis; antiviral treatment; Nosemosis
Mathematics Subject Classification: 34D20, 34D23, 37N25, 49J15, 92B05, 92D25, 93A30

1. Introduction

The decline of global honeybee (*Apis mellifera*) populations has garnered substantial scientific and agricultural concern due to these pollinators' crucial role in maintaining the ecosystem diversity and ensuring agricultural productivity. Among the multiple biotic stressors that affect honeybees, one of the most pervasive is the microsporidian disease known as Nosemosis, which is primarily caused by two intracellular fungal species, *Nosema apis* and *Nosema ceranae*. First described in the early 1900s, *N. apis* was traditionally regarded as the principal etiological agent of Nosemosis in the European honeybee. However, the emergence and global spread of the Asian parasite *N. ceranae*, initially associated with the Eastern honeybee (*Apis cerana*), have reshaped the epidemiology of this infection in apiculture [1–3] that are extended recently to reflect the influence of seasonality [4, 5]. The parasitic invasion of *N. ceranae* has led to a severe reduction in colony productivity, longevity, and in some cases, colony collapse [6, 7]. Nosemosis is characterized by spore ingestion through trophallactic behavior, spore germination within the midgut epithelial cells, and dissemination of the pathogen through feces, which perpetuates environmental contamination. Numerous experimental studies have demonstrated that infection can impair the immune system, reduce the foraging efficiency, disrupt the energy metabolism, and alter the gut microbiota composition [8–10]. Furthermore, *N. ceranae* exhibits distinct thermal and physiological tolerances compared to *N. apis*, thereby enabling its persistence under warmer environmental conditions and suggesting its potential advantage under global climate change [11].

In recent decades, mathematical modeling has become a critical tool to understand the disease transmission and population dynamics of honeybees. Early compartmental models explored demographic changes under different stressors, including pathogens, pesticides, and mites [12–14] that can reflect age structure influence [15]. With the advent of bio-epidemiological data, these models have been refined to capture latency periods, environmental contamination, and host-parasite interactions. For instance, Dénes and Ibrahim [16] analyzed the dynamics of colonies infested by virus-carrying Varroa mites, thus emphasizing the significance of within-colony infection feedbacks. Similarly, El Hajji et al. [17, 18] incorporated environmental seasonality to reveal periodic oscillations in honeybee-parasite interactions, thereby highlighting the need to integrate temporal heterogeneity into epidemic frameworks. Distributed delay models, which generalize classical delay-differential systems, have been widely used in epidemic modeling for their biological realism [19, 20]. Such methods capture the variability in incubation and maturation times that fixed delays cannot represent. These approaches have been applied to diseases such as Zika virus [21], and malaria [22]; however, their application to honeybee Nosemosis remains limited. Previous Nosema models often assumed instantaneous transitions or constant infection rates, which neglects the inherent stochasticity and variability of latency and infectious stages. Additionally, few studies have explored the role of inter-colony interactions—a critical epidemiological driver in apiaries where multiple colonies share foraging resources and pathogen reservoirs.

This study addresses these research gaps by developing a comprehensive mathematical model that jointly considers (i) the co-infection dynamics of two honeybee colonies exposed to dual Nosema species, (ii) the biological realism introduced via distributed delays, and (iii) the influence of antiviral treatment interventions. Our model introduces an environmental pathogen pool shared by the colonies, thus representing a realistic mechanism of indirect transmission. The distributed time delays capture

crucial biological processes, including parasite maturation, latency, and spore germination periods. Moreover, by integrating the treatment efficacy as a control parameter, the model provides quantitative thresholds for successful infection mitigation and eradication. A stability analysis is conducted using rigorous Lyapunov functionals and LaSalle's Invariance Principle, thus allowing us to characterize the global asymptotic behavior of the equilibria. The theoretical results are complemented by numerical simulations to validate the analytical predictions and visualize disease extinction or persistence scenarios under varying parameter regimes.

The remainder of this paper is organized as follows: Section 2 presents the formulation of the dual-target delayed model, thereby describing the biological and epidemiological assumptions underlying the model's compartments; Section 3 analyzes the system without distributed delays, thereby providing expressions for the basic reproduction number R_0 and establishing the existence and global stability of the disease-free and endemic equilibria; Section 4 extends the analysis by incorporating distributed delays, deriving the delayed basic reproduction number R_0^d, and demonstrating global asymptotic stability through Lyapunov functionals; Section 5 provides numerical experiments, sensitivity analyses, and treatment simulations to highlight the quantitative behavior of the model; and finally, Section 6 concludes the paper with remarks on the biological implications, limitations, and directions for future research.

2. Derivation of the mathematical model

In this study, we consider a system composed of two distinct honeybee colonies, denoted as Colonies 1 and 2, which share a common natural foraging and living environment. Each colony is structured into several epidemiological compartments that represent the different health states of the bees with respect to Nosema infection (Figure 1). This compartmentalization allows us to capture the progression of the disease within and between the colonies, as well as the environmental dynamics of the pathogen.

Specifically, for each colony, the bee population is subdivided into the following classes:

- **Susceptible (healthy) bees**: These are individuals free of infection and capable of becoming infected. We denote susceptible bees in Colony 1 by $S_1(t)$ and in Colony 2 by $S_2(t)$.
- **Latently infected bees**: Bees that have been exposed to the Nosema pathogen but are in the latent phase, during which they harbor the parasite without yet being infectious. These are represented by $L_1(t)$ and $L_2(t)$ for Colonies 1 and 2, respectively.
- **Actively infected bees**: These are individuals who have progressed from latency to an infectious state, and are capable of shedding spores and contributing to disease transmission. These compartments are denoted by $I_1(t)$ and $I_2(t)$, respectively.

In addition to the host compartments, we introduce an environmental compartment, $P(t)$, which quantifies the concentration of Nosema spores in the shared environment. This term accounts for the pathogen load shed by infected bees, which mediates the indirect transmission between and within colonies.

The model is grounded on several biological and epidemiological assumptions, which are summarized as follows:

1. **Population dynamics:** Susceptible bees in each colony are replenished at constant recruitment

rates, Λ_1 for Colony 1 and Λ_2 for Colony 2, thereby incorporating birth and immigration processes. Natural mortality acts on all compartments at rates m_1 and m_2 for Colonies 1 and 2, respectively.

2. **Disease transmission:** The infection process occurs through an indirect contact with the environmental pathogen pool $P(t)$. Susceptible bees become latently infected at rates proportional to the product of the susceptible population and the pathogen concentration, with transmission coefficients β_1 and β_2 for each colony.
3. **Latency and Infection progression:** The transition from latent to actively infected stages occurs at incubation rates ζ_1 and ζ_2. The latent and infectious stages have associated average durations, which are inversely related to these rates and mortality rates, thus reflecting the biological delay inherent in parasite development.
4. **Pathogen shedding:** Infectious bees shed Nosema spores into the environment at colony-specific rates k_1 and k_2, thus contributing to the environmental pathogen load $P(t)$.
5. **Environmental decay:** The environmental spores decay or are cleared at a rate m, thus representing natural degradation or removal mechanisms.
6. **Distributed delays:** To realistically represent the biological timing of infection and parasite maturation, we incorporate distributed delays through probability density functions $q_i(\tau)$, with support on the intervals $[0, \omega_i]$, for $i = 1, \ldots, 5$. These delay distributions capture the variability in latency periods, reactivation times, and maturation durations rather than assuming fixed delays.
7. Functions $q_i(\tau)$, $i = 1, \cdots, 5$, satisfy $q_i(\tau) > 0$ and

$$\int_0^{\omega_i} q_i(\tau) d\tau = 1, \quad \int_0^{\omega_i} q_i(\tau) e^{l\tau} d\tau < \infty,$$

where $l > 0$. Let us denote $G_i(\tau) = q_i(\tau) e^{-\eta_i \tau}$ and $F_i = \int_0^{\omega_i} G_i(\tau) d\tau, \quad i = 1, \cdots, 5$, which implies that $0 < F_1, \cdots, F_5 \leq 1$.

Here, the functions $q_i(\tau)$ are the probability density functions which characterize the distributed delays, and η_i represent the mortality or clearance rates during the corresponding delay period. The terms $e^{-\eta_i \tau}$ reflect the survival probabilities of bees or spores surviving the delay time τ. The upper limits ω_i denote the maximal delay durations.

The properties of $q_i(\tau)$ ensure the following:

1. The model is well-posed (existence and uniqueness of solutions);
2. the basic reproduction number $\mathscr{R}_0^d$ can be expressed in terms of G_i;
3. Lyapunov functionals can be constructed to prove global stability; and
4. numerical simulations can be performed using specific kernel choices (e.g., Dirac delta, gamma distribution, uniform distribution).

By specifying $q_i(\tau)$ as probability density functions with the given properties, the model realistically captures the variability and losses associated with time delays in environmental pollution dynamics, while maintaining mathematical tractability for the analysis of global dynamics.

Figure 1 captures the intricate host-parasite-environment interactions that govern Nosema dynamics in coexisting honeybee colonies. By incorporating distributed delays, the mathematical model that we propose hereafter accounts for biological realism in the infection timing and parasite development,

which are essential for accurate predictions of disease progression and control. This comprehensive framework lays the foundation for subsequent analytical and numerical investigations into the transmission dynamics of dual Nosema infections, the effects of distributed delays, and potential treatment strategies within multi-colony apiaries.

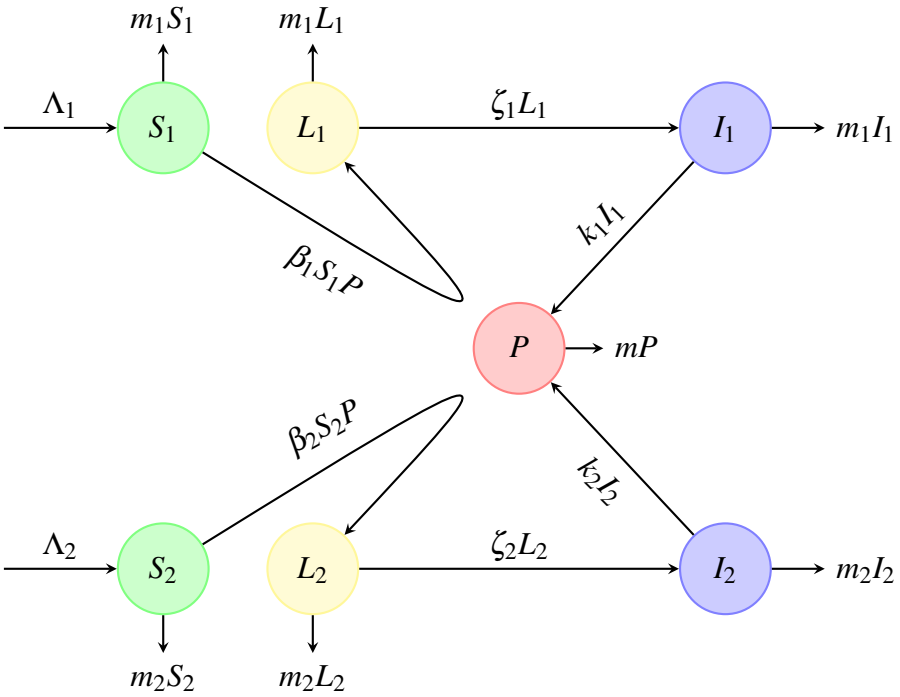

Figure 1. Nosema disease transmission diagram.

Mathematically, the dynamics is described by the following set of integro-differential equations:

$$\begin{cases} \dfrac{dS_1}{dt} = \Lambda_1 - \beta_1 S_1(t)P(t) - m_1 S_1(t), \\ \dfrac{dL_1}{dt} = \beta_1 \displaystyle\int_0^{\omega_1} G_1(\tau)S_1(t-\tau)P(t-\tau)d\tau - (\zeta_1 + m_1)L_1(t), \\ \dfrac{dI_1}{dt} = \zeta_1 \displaystyle\int_0^{\omega_2} G_2(\tau)L_1(t-\tau)d\tau - m_1 I_1(t), \\ \dfrac{dS_2}{dt} = \Lambda_2 - \beta_2 S_2(t)P(t) - m_2 S_2(t), \\ \dfrac{dL_2}{dt} = \beta_2 \displaystyle\int_0^{\omega_3} G_3(\tau)S_2(t-\tau)P(t-\tau)d\tau - (\zeta_2 + m_2)L_2(t), \\ \dfrac{dI_2}{dt} = \zeta_2 \displaystyle\int_0^{\omega_4} G_4(\tau)L_2(t-\tau)d\tau - m_2 I_2(t), \\ \dfrac{dP}{dt} = \displaystyle\int_0^{\omega_5} G_5(\tau)\Big[k_1 I_1(t-\tau) + k_2 I_2(t-\tau)\Big]d\tau - mP(t). \end{cases} \tag{2.1}$$

The parameters and their biological interpretations are summarized in Table 1.

Table 1. Summary of model parameters and their biological meanings.

Parameter	Description
$q_i(\tau)$	Probability density functions for distributed delays ($i = 1,\ldots,5$)
η_i	Mortality rates during delay periods ($i = 1,\ldots,5$)
ω_i	Maximum lengths of distributed delay intervals ($i = 1,\ldots,5$)
Λ_1, Λ_2	Recruitment rates of susceptible bees in Colonies 1 and 2
β_1, β_2	Transmission rates of Nosema spores to susceptible bees
ζ_1, ζ_2	Incubation rates from latent to infectious stages
m_1, m_2	Mortality rates of bees in Colonies 1 and 2
k_1, k_2	Spore shedding rates by infectious bees
m	Decay rate of Nosema spores in the environment

The initial conditions for system (2.1) are given by continuous nonnegative functions defined on the interval $[-\tau^*,0]$, where $\tau^* = \max(\omega_1,\ldots,\omega_5)$:

$$\begin{aligned} &S_1(\theta) = \phi_1^S(\theta),\ L_1(\theta) = \phi_1^L(\theta),\ I_1(\theta) = \phi_1^I(\theta),\ S_2(\theta) = \phi_2^S(\theta), L_2(\theta) = \phi_2^L(\theta),\\ &I_2(\theta) = \phi_2^I(\theta),\ P(\theta) = \phi^P(\theta),\ \theta \in [-\tau^*,0]. \end{aligned} \tag{2.2}$$

$\phi_1^S, \phi_1^L, \phi_1^I, \phi_2^S, \phi_2^L, \phi_2^I$ and ϕ^P are assumed to be bounded, nonnegative, continuous functions, thus reflecting the initial state of the system.

3. Analysis of the non-delayed model

This section focuses on analyzing the simplified version of the model without distributed delays, thus providing a foundational understanding of the system's dynamics. By assuming constant parameters and omitting time delays, we derive explicit expressions for key epidemiological quantities such as the basic reproduction number $\mathscr{R}_0$. We establish the existence, uniqueness, and global stability of both the disease-free and endemic equilibria, using Lyapunov functions and LaSalle's Invariance Principle. This analysis not only clarifies the threshold behavior governed by $\mathscr{R}_0$, but also sets the stage for the more complex delayed model examined in subsequent sections.
We start by providing the dynamical system without distributed delays as follows:

$$\begin{cases} \dot{S}_1 = \Lambda_1 - \beta_1 S_1 P - m_1 S_1, \\ \dot{L}_1 = \beta_1 S_1 P - (\zeta_1 + m_1) L_1, \\ \dot{I}_1 = \zeta_1 L_1 - m_1 I_1, \\ \dot{S}_2 = \Lambda_2 - \beta_2 S_2 P - m_2 S_2, \\ \dot{L}_2 = \beta_2 S_2 P - (\zeta_2 + m_2) L_2, \\ \dot{I}_2 = \zeta_2 L_2 - m_2 I_2, \\ \dot{P} = k_1 I_1 + k_2 I_2 - mP, \end{cases} \tag{3.1}$$

with initial condition $(S_1^0, L_1^0, I_1^0, S_2^0, L_2^0, I_2^0, P^0) \in \mathbb{R}_+^7$.

3.1. Biological feasible domain

In this section, we focus on establishing the biological feasibility of the mathematical model developed to describe the dynamics of honeybee colonies affected by Nosema infections. Specifically,

we analyze the system's behavior under the assumption of constant parameters and without the incorporation of distributed delays. Our aim is to demonstrate that the model's trajectories remain within biologically realistic bounds, thereby ensuring that all populations—healthy, latently infected, and actively infected bees—remain non-negative over time. By defining the biologically feasible region and proving its attractiveness, we lay a solid foundation to understand the system's dynamics and the conditions under which disease-free and endemic equilibria can exist. The biologically feasible region of the dynamics (3.1), denoted here by Σ, is given by the following:

$$\Sigma = \left\{ (S_1, L_1, I_1, S_2, L_2, I_2, P) \in \mathbb{R}^7_+ : S_1 + L_1 + I_1 = \frac{\Lambda_1}{m_1},\ S_2 + L_2 + I_2 = \frac{\Lambda_2}{m_2},\ P \leq \frac{k_1\Lambda_1}{mm_1} + \frac{k_2\Lambda_2}{mm_2} \right\}.$$

Note that the set Σ is positively attracting all trajectories of dynamics (3.1) according to the following results.

Lemma 1. *Σ is a positively invariant, attracting, and compact set for the dynamics of* (3.1).

Proof. By applying the classical theory of functional differential equations [23], system (3.1) with the initial condition in $\mathbb{R}^7_+$ admits a unique solution for $t \geq 0$. Since we have $\dot{S}_1 \mid_{S_1=0} = \Lambda_1 > 0$, $\dot{L}_1 \mid_{L_1=0} = \beta_1 S_1 P > 0$, $\dot{I}_1 \mid_{I_1=0} = \zeta_1 L_1 > 0$, $\dot{S}_2 \mid_{S_2=0} = \Lambda_2 > 0$, $\dot{L}_2 \mid_{L_2=0} = \beta_2 S_2 P > 0$, $\dot{I}_2 \mid_{I_2=0} = \zeta_2 L_2 > 0$, and $\dot{P} \mid_{P=0} = k_1 I_1 + k_2 I_2 > 0$. Therefore, $\mathbb{R}^7_+$ is invariant by the dynamics of (3.1). Let us denote the sizes of the total bees' compartments from the first and second beehives by $T_1 := S_1 + L_1 + I_1$ and $T_2 := S_2 + L_2 + I_2$, respectively. From the dynamics of (3.1), we have $\dot{T}_1 = \Lambda_1 - m_1 S_1 - m_1 L_1 - m_1 I_1 = m_1(\frac{\Lambda_1}{m_1} - T_1)$. Hence, $T_1 = S_1 + L_1 + I_1 = \frac{\Lambda_1}{m_1}$ if $T_1(0) = S_1(0) + L_1(0) + I_1(0) = \frac{\Lambda_1}{m_1}$. Similarly, $\dot{T}_2 = S_2 + L_2 + I_2 = \Lambda_2 - m_2 S_2 - m_2 L_2 - m_2 I_2 = m_2(\frac{\Lambda_2}{m_2} - T_2)$. Hence, $T_2 = S_2 + L_2 + I_2 = \frac{\Lambda_2}{m_2}$ if $T_2(0) = S_2(0) + L_2(0) + I_2(0) = \frac{\Lambda_2}{m_2}$. Similarly, $\dot{P} = k_1 I_1 + k_2 I_2 - mP \leq \frac{k_1\Lambda_1}{m_1} + \frac{k_2\Lambda_2}{m_2} - mP$. Hence, $P \leq \frac{k_1\Lambda_1}{mm_1} + \frac{k_2\Lambda_2}{mm_2}$ if $P(0) \leq \frac{k_1\Lambda_1}{mm_1} + \frac{k_2\Lambda_2}{mm_2}$. □

3.2. Basic reproduction number and equilibria

Now, we will calculate the basic reproduction number, denoted as $\mathscr{R}_0$, for the system described in (3.1) using the next generation matrix [24]. First, we must identify the steady state free of Nosema disease, which has the form $\mathscr{E}_0 = \left(\frac{\Lambda_1}{m_1}, 0, 0, \frac{\Lambda_2}{m_2}, 0, 0, 0\right)$. All equations of (3.1), except the first and the fourth one, characterize the emergence of new infections and the transitions among infected individuals. To build the next generation matrix, we define matrix F to represent the rate at which new infections occur in these equations, while matrix V reflects the rate of movement of individuals into and out of the various compartments. Then the non-negative matrix F and the non-singular matrix V are specified as follows:

$$F = \begin{bmatrix} 0 & 0 & 0 & 0 & \beta_1 \frac{\Lambda_1}{m_1} \\ 0 & 0 & 0 & 0 & \beta_2 \frac{\Lambda_2}{m_2} \\ 0 & 0 & 0 & 0 & 0 \\ 0 & 0 & 0 & 0 & 0 \\ 0 & 0 & 0 & 0 & 0 \end{bmatrix} \text{ and } V = \begin{bmatrix} \zeta_1 + m_1 & 0 & 0 & 0 & 0 \\ 0 & \zeta_2 + m_2 & 0 & 0 & 0 \\ -\zeta_1 & 0 & m_1 & 0 & 0 \\ 0 & -\zeta_2 & 0 & m_2 & 0 \\ 0 & 0 & -k_1 & -k_2 & m \end{bmatrix}.$$

The basic reproduction number for dynamics (3.1) is defined as the spectral radius of the next generation matrix FV^{-1}, which is provided as follows:

$$\mathscr{R}_0 = \frac{k_1\beta_1\zeta_1\Lambda_1}{mm_1^2(\zeta_1+m_1)} + \frac{k_2\beta_2\zeta_2\Lambda_2}{mm_2^2(\zeta_2+m_2)} = \mathscr{R}_{01} + \mathscr{R}_{02}. \tag{3.2}$$

The structure of the basic reproduction number in Eq (3.2) reveals a crucial feature of environmentally transmitted diseases in interconnected populations. Here, $\mathscr{R}_0$ is not merely an average over the two colonies but a sum of colony-specific contributions ($\mathscr{R}_{01} + \mathscr{R}_{02}$).

Biological interpretation: This additive form arises because the environmental spore pool (P) acts as a common infectious reservoir. A single infection in either colony contributes spores to this shared reservoir. Then these spores pose a transmission risk to susceptible bees in both colonies. $\mathscr{R}_{01}$ represents the average number of secondary infections (in either colony) generated over the lifetime of an infected bee that originates from Colony 1, mediated through the environmental reservoir. Similarly, $\mathscr{R}_{02}$ represents the contribution from an infection that originates in Colony 2.

Epidemiological Consequence: The additive property has a critical implication for disease control: An infection introduced into either colony fully contributes to the overall epidemic potential of the entire system. Even if one colony is highly resistant (e.g., $\mathscr{R}_{01} \ll 1$), then a sufficiently high force of infection from the other colony ($\mathscr{R}_{02} > 1$) can maintain $\mathscr{R}_0 > 1$, thus leading to endemic disease in both colonies through the contaminated environment. This models the real-world observation in apiaries that a single diseased hive can act as a source of infection for neighboring hives. In contrast, for models with only direct (bee-to-bee) transmission between colonies, $\mathscr{R}_0$ would typically be a more complex function (e.g., the spectral radius of a next-generation matrix) and not a simple sum. Here, the additive form here is a hallmark of indirect, common-source transmissions.

The additive $\mathscr{R}_0$ is a property of the coupling structure (two sources, one shared sink), not just the sum of two independent populations. It is the correct threshold for the coupled system as modeled. If the system structure changes (by merging), then the threshold changes. This is a strength of the model when applied to separate hives that share a landscape, but it also defines the model's limits.

Theorem 1. *If $\mathscr{R}_0 > 1$, then* (3.1) *admits a unique endemic steady state.*

This theorem confirms the intuitive threshold behavior: a unique endemic steady state exists if and only if $\mathscr{R}_0 > 1$. It guarantees that when the disease can invade, it will stabilize at a predictable, positive level rather than growing without bound or oscillating indefinitely.

Proof. Let the endemic steady state of (3.1) be denoted by $\mathscr{E}^* = (S_1^*, S_2^*, L_1^*, L_2^*, I_1^*, I_2^*, P^*)$. This equilibrium is determined by solving the following two sub-systems of equations:

$$\begin{cases} \Lambda_1 - \beta_1 S_1^* P^* - m_1 S_1^* = 0, \\ \beta_1 S_1^* P^* - (\zeta_1 + m_1) L_1^* = 0, \\ \zeta_1 L_1^* - m_1 I_1^* = 0, \end{cases} \tag{3.3}$$

$$\begin{cases} \Lambda_2 - \beta_2 S_2^* P^* - m_2 S_2^* = 0, \\ \beta_2 S_2^* P^* - (\zeta_2 + m_2) L_2^* = 0, \\ \zeta_2 L_2^* - m_2 I_2^* = 0, \end{cases} \tag{3.4}$$

and

$$k_1 I_1^* + k_2 I_2^* - m P^* = 0. \tag{3.5}$$

We obtain the following:

$$L_1^* = \frac{m_1}{\zeta_1} I_1^*,\ L_2^* = \frac{m_2}{\zeta_2} I_2^*,\ P^* = \frac{k_1 I_1^* + k_2 I_2^*}{m}. \tag{3.6}$$

Substituting (3.6) into the second equations of (3.3) and (3.4) leads to the following:

$$\left(\frac{\beta_1 k_1 S_1^*}{m} - \frac{m_1(\zeta_1+m_1)}{\zeta_1}\right) I_1^* + \left(\frac{\beta_2 k_2 S_2^*}{m} - \frac{m_2(\zeta_2+m_2)}{\zeta_2}\right) I_2^* = 0. \tag{3.7}$$

We can write the following:

$$\frac{m_1(\zeta_1+m_1)}{\zeta_1}\Big(\frac{\beta_1 k_1 S_1^*}{m m_1(\zeta_1+m_1)} - 1\Big) I_1^* + \frac{m_2(\zeta_2+m_2)}{\zeta_2}\Big(\frac{\beta_2 k_2 S_2^*}{m m_2(\zeta_2+m_2)} - 1\Big) I_2^* = 0. \tag{3.8}$$

Equation (3.8) implies that either $I_1^* = I_2^* = 0$, or that $S_1^* = \dfrac{m m_1(\zeta_1+m_1)}{\beta_1 k_1 \zeta_1} = \dfrac{\Lambda_1}{m_1 \mathscr{R}_{01}}$ and $S_2^* = \dfrac{m m_2(\zeta_2+m_2)}{\beta_2 k_2 \zeta_2} = \dfrac{\Lambda_2}{m_2 \mathscr{R}_{02}}$. From the first equations of (3.3) and (3.4), we have $\Big(\Lambda_1 - \beta_1 \dfrac{\Lambda_1}{m_1 \mathscr{R}_{01}} \dfrac{k_1}{m} I_1^* - \dfrac{\Lambda_1}{\mathscr{R}_{01}}\Big) + \Big(\Lambda_2 - \beta_2 \dfrac{\Lambda_2}{m_2 \mathscr{R}_{02}} \dfrac{k_2}{m} I_2^* - \dfrac{\Lambda_2}{\mathscr{R}_{02}}\Big) = 0$, and this gives $I_1^* = \dfrac{m m_1 \mathscr{R}_{01}}{\beta_1 k_1}\Big(1 - \dfrac{1}{\mathscr{R}_{01}}\Big)$ and $I_2^* = \dfrac{m m_2 \mathscr{R}_{02}}{\beta_2 k_2}\Big(1 - \dfrac{1}{\mathscr{R}_{02}}\Big)$. From (3.6), we have $L_1^* = \dfrac{m m_1^2 \mathscr{R}_{01}}{\beta_1 k_1 \zeta_1}\Big(1 - \dfrac{1}{\mathscr{R}_{01}}\Big)$, $L_2^* = \dfrac{m m_2^2 \mathscr{R}_{02}}{\beta_2 k_2 \zeta_2}\Big(1 - \dfrac{1}{\mathscr{R}_{02}}\Big)$, and $P^* = \dfrac{m_1 \mathscr{R}_{01}}{\beta_1}\Big(1 - \dfrac{1}{\mathscr{R}_{01}}\Big) + \dfrac{m_2 \mathscr{R}_{02}}{\beta_2}\Big(1 - \dfrac{1}{\mathscr{R}_{02}}\Big)$. As we can note, $\mathscr{E}^*$ exists whenever $S_1^* > 0$, $S_2^* > 0$, $L_1^* > 0$, $L_2^* > 0$, $I_1^* > 0$, $I_2^* > 0$, and $P^* > 0$, and this only feasible if $\mathscr{R}_0 > 1$. Therefore, we deduce that the endemic equilibrium point $\mathscr{E}^*$ exists, and is unique only if $\mathscr{R}_0 > 1$. □

Now, we will assess the global stability of both the Nosema disease-free equilibrium and the endemic steady state. This analysis of global stability will be conducted through Lyapunov's theory.

3.3. Global stability of equilibria

In this section, we will investigate the global stability of the equilibria established in the previous analyses. Specifically, we aim to determine the conditions under which the disease-free equilibrium and the endemic steady state are globally asymptotically stable. To achieve this, we will employ Lyapunov's stability theory, which provides a robust framework to assess the long-term behavior of dynamical systems. By defining appropriate Lyapunov functions for both equilibria, we will demonstrate how variations in the basic reproduction number, $\mathscr{R}_0$, influence the stability outcomes. This analysis is crucial to understand the potential for disease eradication or persistence within honeybee colonies under the modeled conditions.

Theorem 2. *If $\mathscr{R}_0 \leq 1$, then $\mathscr{E}_0$ is globally asymptotically stable.*

This is a powerful eradication result. It proves that if $\mathscr{R}_0 \leq 1$, then the disease will die out from any initial condition within the biologically feasible set. The proof constructs an explicit Lyapunov function, thereby providing a rigorous guarantee for disease elimination when control measures push $\mathscr{R}_0$ below unity.

Proof. Let us consider the candidate Lyapunov function:

$$\begin{aligned}\mathscr{L}_0 &= \zeta_1 \frac{k_1}{m_1}(m_2+\zeta_2)L_1 + \frac{k_1}{m_1}(m_1+\zeta_1)(m_2+\zeta_2)I_1 + \zeta_2 \frac{k_2}{m_2}(m_1+\zeta_1)L_2 \\ &\quad + \frac{k_2}{m_2}(m_2+\zeta_2)(m_1+\zeta_1)I_2 + (m_1+\zeta_1)(m_2+\zeta_2)P.\end{aligned}$$

The Lyapunov functional $\mathscr{F}_0$ is defined on the biologically feasible set Σ — a positively invariant, bounded subset of $\mathbb{R}^7_+$. It maps states in Σ to nonnegative real numbers, is smooth on the interior of Σ, and only equals to zero at the disease-free equilibrium $\mathscr{E}_0$. This ensures that the Lyapunov analysis is performed in a region that is both biologically realistic and mathematically well-posed.

By differentiating $\mathscr{L}_0$ along the trajectories of the dynamics of (3.1), we obtain the following:

$$\begin{aligned}\dot{\mathscr{L}}_0 &= \zeta_1\frac{k_1}{m_1}(m_2+\zeta_2)\dot{L}_1+\frac{k_1}{m_1}(m_1+\zeta_1)(m_2+\zeta_2)\dot{I}_1+\zeta_2\frac{k_2}{m_2}(m_1+\zeta_1)\dot{L}_2\\ &\quad+\frac{k_2}{m_2}(m_2+\zeta_2)(m_1+\zeta_1)\dot{I}_2+(m_1+\zeta_1)(m_2+\zeta_2)\dot{P}\\ &= m(m_1+\zeta_1)(m_2+\zeta_2)\left[\frac{\beta_1\zeta_1k_1S_1}{mm_1(m_1+\zeta_1)}+\frac{\beta_2\zeta_2k_2S_2}{mm_2(m_2+\zeta_2)}-1\right]P.\end{aligned}$$

Since $S_1 \leq \dfrac{\Lambda_1}{m_1}$ and $S_2 \leq \dfrac{\Lambda_2}{m_2}$, it follows that

$$\frac{\beta_1\zeta_1k_1S_1}{mm_1(m_1+\zeta_1)}+\frac{\beta_2\zeta_2k_2S_2}{mm_2(m_2+\zeta_2)} \leq \frac{\beta_1\zeta_1k_1\Lambda_1}{mm_1^2(m_1+\zeta_1)}+\frac{\beta_2\zeta_2k_2\Lambda_2}{mm_2^2(m_2+\zeta_2)}=\mathscr{R}_0.$$

Then the derivative satisfies the following:

$$\dot{\mathscr{L}}_0 \leq m(m_1+\zeta_1)(m_2+\zeta_2)(\mathscr{R}_0-1)P.$$

Thus, if $\mathscr{R}_0 \leq 1$, then, $\dot{\mathscr{L}}_0 \leq 0$. When $\mathscr{R}_0 < 1$, then, $\dot{\mathscr{L}}_0 = 0$ yields $P = 0$. Therefore, it can be deduced from system (3.1) that, as $t \to \infty$, $L_1 \to 0$, $L_2 \to 0$, $I_1 \to 0$, $I_2 \to 0$, $S_1 \to \dfrac{\Lambda_1}{m_1}$, and $S_2 \to \dfrac{\Lambda_2}{m_2}$. Thus, the invariant set for which $\dot{\mathscr{L}}_0 = 0$ is the singleton $\left\{\mathscr{E}_0 = \left(\dfrac{\Lambda_1}{m_1},0,0,\dfrac{\Lambda_2}{m_2},0,0,0\right)\right\}$. By using Lasalle's Invariance Principle [25], we deduce that any solution of the dynamics of (3.1) with initial conditions in Σ, converges to $\mathscr{E}_0$ as $t \to \infty$. Thus, the equilibrium point $\mathscr{E}_0$ is globally asymptotically stable once $\mathscr{R}_0 < 1$. When $\mathscr{R}_0 = 1$, $\dot{\mathscr{L}}_0 = 0$ implies either $P = 0$, or

$$1 = \frac{\beta_1\zeta_1k_1S_1}{mm_1(m_1+\zeta_1)}+\frac{\beta_2\zeta_2k_2S_2}{mm_2(m_2+\zeta_2)} \leq \frac{\beta_1\zeta_1k_1\Lambda_1}{mm_1^2(m_1+\zeta_1)}+\frac{\beta_2\zeta_2k_2\Lambda_2}{mm_2^2(m_2+\zeta_2)}=\mathscr{R}_0.$$

The latter case yields $S_1 = \dfrac{\Lambda_1}{m_1}$, $S_2 = \dfrac{\Lambda_2}{m_2}$ and, consequently, $L_1 = I_1 = L_2 = I_2 = P = 0$. Therefore, the invariant set for which $\dot{\mathscr{L}}_0 = 0$ is the singleton $\mathscr{E}_0 = \left(\dfrac{\Lambda_1}{m_1},0,0,\dfrac{\Lambda_2}{m_2},0,0,0\right)$. Therefore, the steady state $\mathscr{E}_0$ is globally asymptotically stable if $\mathscr{R}_0 = 1$. □

Theorem 3. *If $\mathscr{R}_0 > 1$, then the endemic steady state of the dynamics of* (3.1)*, $\mathscr{E}^*$, exists, and is globally asymptotically stable.*

This theorem completes the global stability picture. When $\mathscr{R}_0 > 1$, not only does an endemic state exist (Theorem 1), but it attracts all trajectories. This means the disease is predicted to persist at a stable endemic level, irrespective of the initial number of infected bees, thus highlighting the robustness of the endemic state once established.

Proof. Let us define the nonnegative function $\Phi(X) = X - 1 - \ln X$ that only vanishes at $X = 1$, and consider a candidate Lyapunov function $\mathscr{F}^*(S_1, L_1, I_1, S_2, L_2, I_2, P)$ as follows

$$\begin{aligned}\mathscr{F}^* &= S_1^*\Phi\left(\frac{S_1}{S_1^*}\right) + L_1^*\Phi\left(\frac{L_1}{L_1^*}\right) + \frac{m_1+\zeta_1}{\zeta_1}I_1^*\Phi\left(\frac{I_1}{I_1^*}\right) + \frac{k_2 m_1\zeta_2(m_1+\zeta_1)}{k_1 m_2\zeta_1(m_2+\zeta_2)}S_2^*\Phi\left(\frac{S_2}{S_2^*}\right)\\ &\quad + \frac{k_2 m_1\zeta_2(m_1+\zeta_1)}{k_1 m_2\zeta_1(m_2+\zeta_2)}L_2^*\Phi\left(\frac{L_2}{L_2^*}\right) + \frac{k_2 m_1(m_1+\zeta_1)}{k_1 m_2\zeta_1}I_2^*\Phi\left(\frac{I_2}{I_2^*}\right) + \frac{m_1(m_1+\zeta_1)}{k_1\zeta_1}P^*\Phi\left(\frac{P}{P^*}\right).\end{aligned}$$

The Lyapunov functional $\mathscr{F}^*$ is defined on the biologically feasible set Σ. It maps states in Σ to nonnegative real numbers, is smooth on the interior of Σ, and only equals to zero at the disease-free equilibrium $\mathscr{E}^*$.

We calculate $\dfrac{d\mathscr{F}^*}{dt}$ along the trajectories of dynamics (3.1) to obtain the following:

$$\begin{aligned}\frac{d\mathscr{F}^*}{dt} &= \left(1-\frac{S_1^*}{S_1}\right)(\Lambda_1 - m_1S_1 - \beta_1S_1P) + \left(1-\frac{L_1^*}{L_1}\right)(\beta_1S_1P - (m_1+\zeta_1)L_1)\\ &\quad + \frac{m_1+\zeta_1}{\zeta_1}\left(1-\frac{I_1^*}{I_1}\right)(\zeta_1L_1 - m_1I_1) + \frac{k_2m_1\zeta_2(m_1+\zeta_1)}{k_1m_2\zeta_1(m_2+\zeta_2)}\left(1-\frac{S_2^*}{S_2}\right)(\Lambda_2 - m_2S_2 - \beta_2S_2P)\\ &\quad + \frac{k_2m_1\zeta_2(m_1+\zeta_1)}{k_1m_2\zeta_1(m_2+\zeta_2)}\left(1-\frac{L_2^*}{L_2}\right)(\beta_2S_2P - (m_2+\zeta_2)L_2)\\ &\quad + \frac{k_2m_1(m_1+\zeta_1)}{k_1m_2\zeta_1}\left(1-\frac{I_2^*}{I_2}\right)(\zeta_2L_2 - m_2I_2) + \frac{m_1(m_1+\zeta_1)}{k_1\zeta_1}\left(1-\frac{P^*}{P}\right)(k_1I_1 + k_2I_2 - mP).\end{aligned}$$

By using the equilibrium equalities

$$\begin{aligned}&\Lambda_1 = m_1S_1^* + \beta_1S_1^*P^*,\ \Lambda_2 = m_2S_2^* + \beta_2S_2^*P^*,\ k_1I_1^* + k_2I_2^* = mP^*,\\ &\beta_1S_1^*P^* = (m_1+\zeta_1)L_1^*, \zeta_1L_1^* = m_1I_1^*,\ \beta_2S_2^*P^* = (m_2+\zeta_2)L_2^*, \zeta_2L_2^* = m_2I_2^*,\end{aligned}$$

we get

$$m_1I_1^* = \zeta_1L_1^* = \frac{\zeta_1\beta_1S_1^*P^*}{(m_1+\zeta_1)}, m_2I_2^* = \zeta_2L_2^* = \frac{\zeta_2\beta_2S_2^*P^*}{(m_2+\zeta_2)},$$

and

$$\begin{aligned}\frac{d\mathscr{F}^*}{dt} &= \left(1-\frac{S_1^*}{S_1}\right)(m_1S_1^* - m_1S_1) + \beta_1S_1^*P^*\left(1-\frac{S_1^*}{S_1}\right) - \beta_1S_1P\frac{L_1^*}{L_1} + \beta_1S_1^*P^*\\ &\quad - \beta_1S_1^*P^*\frac{I_1^*}{I_1}\frac{L_1}{L_1^*} + \beta_1S_1^*P^* + \frac{k_2m_1\zeta_2(m_1+\zeta_1)}{k_1m_2\zeta_1(m_2+\zeta_2)}\left(1-\frac{S_2^*}{S_2}\right)(m_2S_2^* - m_2S_2)\\ &\quad + \frac{k_2m_1\zeta_2(m_1+\zeta_1)}{k_1m_2\zeta_1(m_2+\zeta_2)}\beta_2S_2^*P^*\left(1-\frac{S_2^*}{S_2}\right) - \frac{k_2m_1\zeta_2(m_1+\zeta_1)}{k_1m_2\zeta_1(m_2+\zeta_2)}\beta_2S_2^*P^*\frac{S_2PL_2^*}{S_2^*P^*L_2}\\ &\quad + \frac{k_2m_1\zeta_2(m_1+\zeta_1)}{k_1m_2\zeta_1(m_2+\zeta_2)}\beta_2S_2^*P^* - \frac{k_2m_1\zeta_2(m_1+\zeta_1)}{k_1m_2\zeta_1(m_2+\zeta_2)}\beta_2S_2^*P^*\frac{I_2^*}{I_2}\frac{L_2}{L_2^*}\\ &\quad + \frac{k_2m_1\zeta_2(m_1+\zeta_1)}{k_1m_2\zeta_1(m_2+\zeta_2)}\beta_2S_2^*P^* - \beta_1S_1^*P^*\frac{I_1}{I_1^*}\frac{P^*}{P} - \frac{k_2m_1\zeta_2(m_1+\zeta_1)}{k_1m_2\zeta_1(m_2+\zeta_2)}\beta_2S_2^*P^*\frac{I_2}{I_2^*}\frac{P^*}{P}\\ &\quad + \beta_1S_1^*P^* + \frac{k_2m_1\zeta_2(m_1+\zeta_1)}{k_1m_2\zeta_1(m_2+\zeta_2)}\beta_2S_2^*P^*.\end{aligned}$$

Therefore,

$$\begin{aligned}\frac{d\mathscr{F}^*}{dt} &= -\frac{m_1(S_1-S_1^*)^2}{S_1}-\frac{k_2m_1\zeta_2(m_1+\zeta_1)}{k_1m_2\zeta_1(m_2+\zeta_2)}\frac{m_2(S_2-S_2^*)^2}{S_2}\\ &+\beta_1S_1^*P^*\left(4-\frac{S_1^*}{S_1}-\frac{I_1P^*}{I_1^*P}-\frac{I_1^*L_1}{I_1L_1^*}-\frac{S_1PL_1^*}{S_1^*P^*L_1}\right)\\ &+\frac{k_2m_1\zeta_2(m_1+\zeta_1)}{k_1m_2\zeta_1(m_2+\zeta_2)}\beta_2S_2^*P^*\left(4-\frac{S_2^*}{S_2}-\frac{I_2P^*}{I_2^*P}-\frac{I_2^*L_2}{I_2L_2^*}-\frac{S_2PL_2^*}{S_2^*P^*L_2}\right).\end{aligned}$$

By applying the relation between the arithmetical and geometrical means

$$\frac{x_1+x_2+\cdots+x_n}{n}\geq\sqrt[n]{x_1x_2\cdots x_n},\ \text{for all } x_1,x_2,\cdots,x_n\geq 0, \tag{3.9}$$

we get

$$4\leq\frac{S_1^*}{S_1}+\frac{I_1P^*}{I_1^*P}+\frac{I_1^*L_1}{I_1L_1^*}+\frac{S_1PL_1^*}{S_1^*P^*L_1}\ \text{and}\ 4\leq\frac{S_2^*}{S_2}+\frac{I_2P^*}{I_2^*P}+\frac{I_2^*L_2}{I_2L_2^*}+\frac{S_2PL_2^*}{S_2^*P^*L_2}.$$

Hence, $\frac{d\mathscr{F}^*}{dt}\leq 0$. Moreover, $\frac{d\mathscr{F}^*}{dt}=0$ if $(S_1,L_1,I_1,S_2,L_2,I_2,P)=(S_1^*,L_1^*,I_1^*,S_2^*,L_2^*,I_2^*,P^*)$. LaSalle's invariance principle indicates that $\mathscr{E}^*$ is globally asymptotically stable when $\mathscr{R}_0>1$. □

The analysis of the non-delayed model provides crucial biological insights into the dynamics of Nosema transmission between two honeybee colonies. The basic reproduction number, $\mathscr{R}_0=\mathscr{R}_{01}+\mathscr{R}_{02}$, acts as a clear threshold to determine the long-term fate of the disease within the apiary. If $\mathscr{R}_0\leq 1$, then the disease-free equilibrium is globally stable, which indicates that the infection will naturally die out as each infected bee, on average, fails to replace itself with a new infection. Conversely, if $\mathscr{R}_0>1$, then the pathogen can successfully invade and persist at an endemic level, thus establishing a stable balance between new infections and the loss of infected individuals. This persistence is characterized by a positive equilibrium where the number of healthy bees is reduced, and a constant level of infection is maintained within the colonies and their shared environment. These findings underscore that effective disease management must aim to reduce $\mathscr{R}_0$ below unity, which can be achieved by targeting key parameters such as transmission rates (β_1,β_2) or spore shedding rates (k_1,k_2), for instance, through improved hive hygiene or treatments that lower the infectiousness of bees.

4. Impact of distributed delays

Having established the foundational dynamics of the system in the absence of distributed delays, we now extend our analysis to incorporate a more biologically realistic framework. This section reintroduces the full model with distributed delays, as defined in system (2.1), to account for the essential time lags inherent in the Nosema infection process. These delays capture the durations of latency, incubation, and parasite maturation, which are critical to accurately model the progression of the disease. We begin by verifying the well-posedness of the model, thus establishing the non-negativity and boundedness of solutions within a biologically feasible domain. Subsequently, we derive the delayed basic reproduction number, $\mathscr{R}_0^d$, and analyze the existence and stability of the system's equilibria. The global stability of both the disease-free and endemic equilibria are rigorously examined

using appropriately constructed Lyapunov functionals, thereby generalizing the results from the non-delayed case and revealing how time delays influence the long-term outcome of the epidemic.

Let us return to the main system (2.1) and start by discussing the existence, positivity, and boundedness of the trajectories.

4.1. Biological feasible domain

Lemma 2. *The dynamics (2.1) with initial conditions (2.2) admits nonnegative and ultimately bounded solutions. Furthermore, the dynamics (2.1) admits an invariant set given by the following:*

$$\Sigma^d = \left\{(S_1,L_1,I_1,S_2,L_2,I_2,P)\in\mathbb{R}^7_+ : \|S_1\|\leq\frac{\Lambda_1}{m_1},\|L_1\|\leq\frac{\Lambda_1}{m_1},\|I_1\|\leq\frac{\zeta_1\Lambda_1}{m_1^2},\|S_2\|\leq\frac{\Lambda_2}{m_2},\|L_2\|\leq\frac{\Lambda_2}{m_2},\right.$$
$$\left.\|I_2\|\leq\frac{\zeta_2\Lambda_2}{m_2^2},\|P\|\leq\frac{k_1\zeta_1\Lambda_1}{mm_1^2}+\frac{k_2\zeta_2\Lambda_2}{mm_2^2}\right\}.$$

Proof. By the classical theory of functional differential equations [23], system (2.1) with initial conditions (2.2) admits a unique solution for $t\geq 0$. Clearly, $\dot{S}_1\mid_{S_1=0}=\Lambda_1>0$, $\dot{S}_2\mid_{S_2=0}=\Lambda_2>0$. Hence, $S_1(t)>0$ and $S_2(t)>0$ for any $t\geq 0$. In addition, we have the following:

$$\begin{aligned}
L_1(t) &= e^{-(m_1+\zeta_1)t}\phi_1^L(0)+\beta_1\int_0^t e^{-(m_1+\zeta_1)(t-\theta)}\int_0^{\omega_1}G_1(\tau)S_1(\theta-\tau)P(\theta-\tau)d\tau d\theta\geq 0,\\
I_1(t) &= e^{-m_1t}\phi_1^I(0)+\zeta_1\int_0^t e^{-m_1(t-\theta)}\int_0^{\omega_2}G_2(\tau)L_1(\theta-\tau)d\tau d\theta\geq 0,\\
L_2(t) &= e^{-(m_2+\zeta_2)t}\phi_2^L(0)+\beta_2\int_0^t e^{-(m_2+\zeta_2)(t-\theta)}\int_0^{\omega_3}G_3(\tau)S_2(\theta-\tau)P(\theta-\tau)d\tau d\theta\geq 0,\\
I_2(t) &= e^{-m_2t}\phi_2^I(0)+\zeta_2\int_0^t e^{-m_2(t-\theta)}\int_0^{\omega_4}G_4(\tau)L_2(\theta-\tau)d\tau d\theta\geq 0,\\
P(t) &= e^{-mt}\phi^P(0)+\int_0^t e^{-m(t-\theta)}\int_0^{\omega_5}G_5(\tau)[k_1I_1(\theta-\tau)+k_2I_2(\theta-\tau)]d\tau d\theta\geq 0,
\end{aligned}$$

for any $t\in[0,\tau^*]$. Therefore, by recursive argumentation, we deduce that

$$(S_1,L_1,I_1,S_2,L_2,I_2,P)(t)\geq 0 \text{ for any } t\geq 0.$$

According to the first equation of dynamics (2.1), we get $\limsup_{t\to\infty}S_1(t)\leq\frac{\Lambda_1}{m_1}$. Let us define the following:

$$\psi_1(t)=\int_0^{\omega_1}G_1(\tau)S_1(t-\tau)d\tau+L_1(t).$$

Then, we obtain the following:

$$\begin{aligned}
\dot{\psi}_1(t) &= \int_0^{\omega_1}G_1(\tau)\dot{S}_1(t-\tau)d\tau+\dot{L}_1(t)\\
&= \int_0^{\omega_1}G_1(\tau)\left[\Lambda_1-m_1S_1(t-\tau)-\beta_1S_1(t-\tau)P(t-\tau)\right]d\tau\\
&\quad+\beta_1\int_0^{\omega_1}G_1(\tau)S_1(t-\tau)P(t-\tau)d\tau-(m_1+\zeta_1)L_1(t)
\end{aligned}$$

$$\begin{aligned} &= \Lambda_1 \int_0^{\omega_1} G_1(\tau)d\tau - m_1 \int_0^{\omega_1} G_1(\tau)S_1(t-\tau)d\tau - (m_1+\zeta_1)L_1(t) \\ &= \Lambda_1 F_1 - m_1 \int_0^{\omega_1} G_1(\tau)S_1(t-\tau)d\tau - (m_1+\zeta_1)L_1(t) \\ &\leq \Lambda_1 - m_1 \left[\int_0^{\omega_1} G_1(\tau)S_1(t-\tau)d\tau + L_1(t)\right] = m_1\left(\frac{\Lambda_1}{m_1} - \psi_1(t)\right). \end{aligned}$$

It follows that $\limsup_{t\to\infty} \psi_1(t) \leq \frac{\Lambda_1}{m_1}$, and then $\limsup_{t\to\infty} L_1(t) \leq \frac{\Lambda_1}{m_1}$. Similarly, we have the following:

$$\dot{I}_1(t) = \zeta_1 \int_0^{\omega_2} G_2(\tau)L_1(t-\tau)d\tau - m_1 I_1(t) \leq \frac{\zeta_1\Lambda_1}{m_1}F_2 - m_1 I_1(t) \leq \frac{\zeta_1\Lambda_1}{m_1} - m_1 I_1(t).$$

It follows that $\limsup_{t\to\infty} I_1(t) \leq \frac{\zeta_1\Lambda_1}{m_1^2}$. Similarly, let us define the following:

$$\psi_2(t) = \int_0^{\omega_3} G_3(\tau)S_2(t-\tau)d\tau + L_2(t).$$

Then, we obtain the following:

$$\begin{aligned} \dot{\psi}_2(t) &= \int_0^{\omega_3} G_3(\tau)\dot{S}_2(t-\tau)d\tau + \dot{L}_2(t) \\ &= \int_0^{\omega_3} G_3(\tau)\left[\Lambda_2 - m_2 S_2(t-\tau) - \beta_2 S_2(t-\tau)P(t-\tau)\right]d\tau \\ &\quad + \beta_2 \int_0^{\omega_3} G_3(\tau)S_2(t-\tau)P(t-\tau)d\tau - (m_2+\zeta_2)L_2(t) \\ &= \Lambda_2 \int_0^{\omega_3} G_3(\tau)d\tau - m_2 \int_0^{\omega_3} G_3(\tau)S_2(t-\tau)d\tau - (m_2+\zeta_2)L_2(t) \\ &\leq \Lambda_2 - m_2\left[\int_0^{\omega_3} G_3(\tau)S_2(t-\tau)d\tau + L_2(t)\right] = \Lambda_2 - m_2\psi_2(t). \end{aligned}$$

It follows that $\limsup_{t\to\infty} \psi_2(t) \leq \frac{\Lambda_2}{m_2}$, and then $\limsup_{t\to\infty} L_2(t) \leq \frac{\Lambda_2}{m_2}$. Note that

$$\dot{Y}_i(t) = \zeta_2 \int_0^{\omega_4} G_4(\tau)L_2(t-\tau)d\tau - m_2 I_2(t) \leq \frac{\zeta_2\Lambda_2}{m_2} - m_2 I_2(t).$$

It follows that $\limsup_{t\to\infty} I_2(t) \leq \frac{\zeta_2\Lambda_2}{m_2^2}$. By the same way, we obtain the following:

$$\begin{aligned} \dot{P}(t) &= \int_0^{\omega_5} G_5(\tau)[k_1 I_1(t-\tau) + k_2 I_2(t-\tau)]d\tau - mP(t) \\ &\leq \left[\frac{k_1\zeta_1}{m_1}\frac{\Lambda_1}{m_1} + \frac{k_2\zeta_2}{m_2}\frac{\Lambda_2}{m_2}\right] - mP(t). \end{aligned}$$

It follows that $\limsup_{t\to\infty} P(t) \leq \frac{k_1\zeta_1\Lambda_1}{mm_1^2} + \frac{k_2\zeta_2\Lambda_2}{mm_2^2}$. Therefore, one deduces that Σ^d is positively invariant w.r.t. system (2.1). □

Next, we will calculate the basic reproduction number and study the existence of equilibria of dynamics (2.1).

4.2. Computation of the basic reproduction number and equilibria

This section analyzes the existence of equilibria for the proposed model. To compute the basic reproduction number, $\mathscr{R}_0^d$, associated with the dual target infection dynamics, we utilize the next-generation matrix approach as described in [24]. In fact, we will prove that $\mathscr{R}_0^d = \mathscr{R}_{01}^d + \mathscr{R}_{02}^d$, where $\mathscr{R}_{01}^d$ and $\mathscr{R}_{02}^d$ denote the total number of newly infected bees in the first and second beehives generated from a single infected bee at the onset of the infection, respectively. The parameter $\mathscr{R}_0^d$ represents the basic reproduction number for the dual-target infection. The basic reproduction number is determined at the disease-free equilibrium point. In our case, the infection-free equilibrium point of system (2.1) is given by $\mathscr{E}_0^d = \left(\frac{\Lambda_1}{m_1}, 0, 0, \frac{\Lambda_2}{m_2}, 0, 0, 0\right)$. The basic reproduction number, $\mathscr{R}_0^d$, is defined as the spectral radius of the next-generation matrix, denoted by $\rho(F_0^d V_0^{d^{-1}})$. In this formulation, F_0^d contains the rates at which new infections occur, while V_0^d captures the rates of transitions between infected compartments. These matrices are derived based on the model structure using the methodology introduced by [24]. The specific forms of F_0^d and V_0^d are given below:

$$F_0^d = \begin{pmatrix} 0 & 0 & 0 & 0 & F_1\beta_1\frac{\Lambda_1}{m_1} \\ 0 & 0 & 0 & 0 & 0 \\ 0 & 0 & 0 & 0 & F_3\beta_2\frac{\Lambda_2}{m_2} \\ 0 & 0 & 0 & 0 & 0 \\ 0 & 0 & 0 & 0 & 0 \end{pmatrix}, \quad V_0^d = \begin{pmatrix} m_1+\zeta_1 & 0 & 0 & 0 & 0 \\ -\zeta_1 F_2 & m_1 & 0 & 0 & 0 \\ 0 & 0 & m_2+\zeta_2 & 0 & 0 \\ 0 & 0 & -\zeta_2 F_4 & m_2 & 0 \\ 0 & -k_1 F_5 & 0 & -k_2 F_5 & m \end{pmatrix}.$$

Therefore,

$$\mathscr{R}_0^d = \rho(F_0^d V_0^{d^{-1}}) = \mathscr{R}_{01}^d + \mathscr{R}_{02}^d,$$

where

$$\mathscr{R}_{01}^d = \frac{k_1\zeta_1\beta_1 F_1 F_2 F_5 \Lambda_1}{m m_1^2(m_1+\zeta_1)} \quad \text{and} \quad \mathscr{R}_{02}^d = \frac{k_2\zeta_2\beta_2 F_3 F_4 F_5 \Lambda_2}{m m_2^2(m_2+\zeta_2)}.$$

Therefore, we obtain the following main result regarding the existence and uniqueness of the equilibria of the system (2.1).

Lemma 3. • *System (2.1) admits an infection-free equilibrium denoted by the following:*

$$\mathscr{E}_0^d = \left(\frac{\Lambda_1}{m_1}, 0, 0, \frac{\Lambda_2}{m_2}, 0, 0, 0\right).$$

• *If $\mathscr{R}_0^d > 1$, then the system (2.1) admits an endemic equilibrium point denoted by the following:*

$$\mathscr{E}_d^* = (S_1^*, L_1^*, I_1^*, S_2^*, L_2^*, I_2^*, P^*).$$

Proof. By setting the time-derivatives to zero, we obtain the following:

$$\begin{cases} 0 &= \Lambda_1 - m_1 S_1 - \beta_1 S_1 P, \\ 0 &= \beta_1 F_1 S_1 P - (m_1+\zeta_1) L_1, \\ 0 &= \zeta_1 F_2 L_1 - m_1 I_1, \\ 0 &= \Lambda_2 - m_2 S_2 - \beta_2 S_2 P, \\ 0 &= \beta_2 F_3 S_2 P - (m_2+\zeta_2) L_2, \\ 0 &= \zeta_2 F_4 L_2 - m_2 I_2, \\ 0 &= F_5(k_1 I_1 + k_2 I_2) - mP. \end{cases}$$

We have the following two cases:

1. If $P = 0$, then the system admits an infection-free equilibrium point as follows:

$$\mathscr{E}_0^d = \left(\frac{\Lambda_1}{m_1}, 0, 0, \frac{\Lambda_2}{m_2}, 0, 0, 0\right).$$

2. If $P \neq 0$, we obtain

$$S_1 = \frac{\Lambda_1}{m_1 + \beta_1 P},\ S_2 = \frac{\Lambda_2}{m_2 + \beta_2 P},\ L_1 = \frac{m_1\beta_1 F_1 \Lambda_1 P}{m_1(m_1+\zeta_1)(m_1+\beta_1 P)},$$
$$I_1 = \frac{\zeta_1\beta_1 F_1 F_2 \Lambda_1 P}{m_1(m_1+\zeta_1)(m_1+\beta_1 P)},\ L_2 = \frac{m_2\beta_2 F_3 \Lambda_2 P}{m_2(m_2+\zeta_2)(m_2+\beta_2 P)},$$
$$I_2 = \frac{\zeta_2\beta_2 F_3 F_4 \Lambda_2 P}{m_2(m_2+\zeta_2)(m_2+\beta_2 P)},$$

and P satisfies the following equation:

$$\frac{k_1\zeta_1\beta_1 F_1 F_2 F_5 \Lambda_1}{m_1(m_1+\zeta_1)(m_1+\beta_1 P)} + \frac{k_2\zeta_2\beta_2 F_3 F_4 F_5 \Lambda_2}{m_2(m_2+\zeta_2)(m_2+\beta_2 P)} - m = 0.$$

Let us consider the function h given by the following:

$$h(P) = \frac{k_1\zeta_1\beta_1 F_1 F_2 F_5 \Lambda_1}{m_1(m_1+\zeta_1)(m_1+\beta_1 P)} + \frac{k_2\zeta_2\beta_2 F_3 F_4 F_5 \Lambda_2}{m_2(m_2+\zeta_2)(m_2+\beta_2 P)} - m.$$

Then, we have the following:

$$\begin{aligned} h(0) &= \frac{k_1\zeta_1\beta_1 F_1 F_2 F_5 \Lambda_1}{m_1^2(m_1+\zeta_1)} + \frac{k_2\zeta_2\beta_2 F_3 F_4 F_5 \Lambda_2}{m_2^2(m_2+\zeta_2)} - m \\ &= m\left(\frac{k_1\zeta_1\beta_1 F_1 F_2 F_5 \Lambda_1}{m m_1^2(m_1+\zeta_1)} + \frac{k_2\zeta_2\beta_2 F_3 F_4 F_5 \Lambda_2}{m m_2^2(m_2+\zeta_2)} - 1\right) \\ &= m\left(\mathscr{R}_0^d - 1\right). \end{aligned}$$

Thus, $h(0) > 0$ when $\mathscr{R}_0^d > 1$. Furthermore, we have $h(P) \to -m < 0$ whenever $P \to \infty$. Moreover,

$$h'(P) = -\left(\frac{k_1\zeta_1\beta_1^2 F_1 F_2 F_5 \Lambda_1}{m_1(m_1+\zeta_1)(m_1+\beta_1 P)^2} + \frac{k_2\zeta_2\beta_2^2 F_3 F_4 F_5 \Lambda_2}{m_2(m_2+\zeta_2)(m_2+\beta_2 P)^2}\right) < 0.$$

Thus, h is a strictly decreasing function of P and hence, if $\mathscr{R}_0^d > 1$, then there exists a unique $P^* \in (0, \infty)$ such that $h(P^*) = 0$. Hence,

$$S_1^* = \frac{\Lambda_1}{m_1 + \beta_1 P^*},\ S_2^* = \frac{\Lambda_2}{m_2 + \beta_2 P^*},\ L_1^* = \frac{\beta_1 F_1 \Lambda_1 P^*}{(m_1+\zeta_1)(m_1+\beta_1 P^*)},$$
$$I_1^* = \frac{\zeta_1\beta_1 F_1 F_2 \Lambda_1 P^*}{m_1(m_1+\zeta_1)(m_1+\beta_1 P^*)}, L_2^* = \frac{\beta_2 F_3 \Lambda_2 P^*}{(m_2+\zeta_2)(m_2+\beta_2 P^*)}, I_2^* = \frac{\zeta_2\beta_2 F_3 F_4 \Lambda_2 P^*}{m_2(m_2+\zeta_2)(m_2+\beta_2 P^*)},$$

where P^* satisfies the following quadratic equation:

$$a{P^*}^2 + bP^* + c = 0, \tag{4.1}$$

where

$$
\begin{aligned}
a &= m\beta_1\beta_2(m_1+\zeta_1)(m_2+\zeta_2) > 0,\\
b &= m(m_2\beta_1+m_1\beta_2)(\zeta_1+m_1)(\zeta_2+m_2)\\
&\quad -\beta_1\beta_2F_5\Big(k_2\zeta_2F_3F_4\frac{\Lambda_2}{m_2}(\zeta_1+m_1)+k_1\zeta_1F_1F_2\frac{\Lambda_1}{m_1}(\zeta_2+m_2)\Big),\\
c &= mm_1m_2(m_1+\zeta_1)(m_2+\zeta_2)\left(1-\mathscr{R}_0^d\right).
\end{aligned}
$$

Clearly, $c<0$ if $\mathscr{R}_0^d>1$. Equation (4.1) admits a unique positive solution given by $P^*=\dfrac{-b+\sqrt{b^2-4ac}}{2a}>0$. For $\mathscr{R}_0^d>1$, we obtain a unique endemic equilibrium point given by $\mathscr{E}_d^*=(S_1^*,L_1^*,I_1^*,S_2^*,L_2^*,I_2^*,P^*)$.

□

4.3. Global stability

In this section, we will focus on the computation of the basic reproduction number, $\mathscr{R}_0^d$, for the model with distributed delays. This parameter is essential to understand the potential for disease spread within the honeybee colonies, as it indicates the average number of secondary infections generated by a single infected individual in a population free of the disease. We will utilize the next generation matrix approach to derive $\mathscr{R}_0^d$ and analyze how the inclusion of distributed delays alters its value compared to the non-delayed scenario. By examining the implications of $\mathscr{R}_0^d$ on the stability of the dynamics (2.1), we aim to provide insights into the dynamics of Nosema infections and their management in honeybee populations. Let us denote by $(S_1,L_1,I_1,S_2,L_2,I_2,P)=(S_1,L_1,I_1,S_2,L_2,I_2,P)(t)$, and $(S_1^\tau,L_1^\tau,I_1^\tau,S_2^\tau,L_2^\tau,I_2^\tau,P^\tau)=(S_1,L_1,I_1,S_2,L_2,I_2,P)(t-\tau)$.

Theorem 4. *The infection-free equilibrium point $\mathscr{E}_0^d$ is globally asymptotically stable once $\mathscr{R}_0^d\le 1$.*

This result generalizes Theorem 2 to the biologically realistic delayed system. It proves that the threshold condition $\mathscr{R}_0^d\le 1$ remains a sharp criterion for global disease eradication, even when accounting for variable incubation and maturation periods. The construction of a Lyapunov functional capable of handling distributed delays is a key technical achievement.

Proof. Let us consider a candidate Lyapunov function $\mathscr{F}_0^d(S_1,L_1,I_1,S_2,L_2,I_2,P)$

$$
\begin{aligned}
\mathscr{F}_0^d &= F_1F_2F_5\frac{\Lambda_1}{m_1}\Phi\left(\frac{m_1S_1}{\Lambda_1}\right)+F_2F_5L_1+F_5\frac{m_1+\zeta_1}{\zeta_1}I_1\\
&\quad +F_3F_4F_5\frac{k_2m_1\zeta_2(m_1+\zeta_1)}{k_1m_2\zeta_1(m_2+\zeta_2)}\frac{\Lambda_2}{m_2}\Phi\left(\frac{m_2S_2}{\Lambda_2}\right)\\
&\quad +F_4F_5\frac{k_2m_1\zeta_2(m_1+\zeta_1)}{k_1m_2\zeta_1(m_2+\zeta_2)}L_2+F_5\frac{k_2m_1(m_1+\zeta_1)}{k_1m_2\zeta_1}I_2+\frac{m_1(m_1+\zeta_1)}{k_1\zeta_1}P\\
&\quad +F_2F_5\beta_1\int_0^{\omega_1}G_1(\tau)\int_{t-\tau}^{t}S_1(\theta)P(\theta)d\theta d\tau\\
&\quad +F_5(m_1+\zeta_1)\int_0^{\omega_2}G_2(\tau)\int_{t-\tau}^{t}L_1(\theta)d\theta d\tau\\
&\quad +F_4F_5\beta_2\frac{k_2m_1\zeta_2(m_1+\zeta_1)}{k_1m_2\zeta_1(m_2+\zeta_2)}\int_0^{\omega_3}G_3(\tau)\int_{t-\tau}^{t}S_2(\theta)P(\theta)d\theta d\tau
\end{aligned}
$$

$$+F_5\frac{k_2m_1\zeta_2(m_1+\zeta_1)}{k_1m_2\zeta_1}\int_0^{\omega_4}G_4(\tau)\int_{t-\tau}^{t}L_2(\theta)d\theta d\tau$$
$$+\frac{m_1(m_1+\zeta_1)}{k_1\zeta_1}\int_0^{\omega_5}G_5(\tau)\int_{t-\tau}^{t}\big(k_1I_1(\theta)+k_2I_2(\theta)\big)d\theta d\tau.$$

The Lyapunov functional $\mathscr{F}_0^d$ is defined on the biologically feasible set Σ^d — a positively invariant, bounded subset of $\mathbb{R}_+^7$. It maps states in Σ^d to nonnegative real numbers, is smooth on the interior of Σ^d, and only equals to zero at the disease-free equilibrium $\mathscr{E}_0^d$. This ensures that the Lyapunov analysis is performed in a region that is both biologically realistic and mathematically well-posed.

We calculate $\frac{d\mathscr{F}_0^d}{dt}$ along the trajectories of the dynamics (2.1) to obtain the following:

$$\begin{aligned}\frac{d\mathscr{F}_0^d}{dt} &= F_1F_2F_5\left(1-\frac{\Lambda_1}{m_1S_1}\right)\dot{S}_1+F_2F_5\dot{L}_1+F_5\frac{m_1+\zeta_1}{\zeta_1}\dot{I}_1\\
&+F_3F_4F_5\frac{k_2m_1\zeta_2(m_1+\zeta_1)}{k_1m_2\zeta_1(m_2+\zeta_2)}\left(1-\frac{\Lambda_2}{m_2S_2}\right)\dot{S}_2+F_4F_5\frac{k_2m_1\zeta_2(m_1+\zeta_1)}{k_1m_2\zeta_1(m_2+\zeta_2)}\dot{L}_2\\
&+F_5\frac{k_2m_1(m_1+\zeta_1)}{k_1m_2\zeta_1}\dot{I}_2+\frac{F_3F_4F_8}{k_2}\frac{m_1(m_1+\zeta_1)}{k_1\zeta_1}\dot{P}\\
&+F_2F_5\beta_1\int_0^{\omega_1}G_1(\tau)(S_1P-S_1^{\tau}P^{\tau})d\tau+F_5(m_1+\zeta_1)\int_0^{\omega_2}G_2(\tau)(L_1-L_1^{\tau})d\tau\\
&+F_4F_5\beta_2\frac{k_2m_1\zeta_2(m_1+\zeta_1)}{k_1m_2\zeta_1(m_2+\zeta_2)}\int_0^{\omega_3}G_3(\tau)(S_2P-S_2^{\tau}P^{\tau})d\tau\\
&+F_5\frac{k_2m_1\zeta_2(m_1+\zeta_1)}{k_1m_2\zeta_1}\int_0^{\omega_4}G_4(\tau)(L_2-L_2^{\tau})d\tau\\
&+\frac{m_1(m_1+\zeta_1)}{k_1\zeta_1}\int_0^{\omega_5}G_5(\tau)\big[k_1(I_1-I_1^{\tau})+k_2(I_2-I_2^{\tau})\big]d\tau.\end{aligned}$$

From the dynamics (2.1), we obtain the following:

$$\begin{aligned}\frac{d\mathscr{F}_0^d}{dt} &= -F_1F_2F_5\frac{m_1}{S_1}\left(S_1-\frac{\Lambda_1}{m_1}\right)^2-F_1F_2F_5\beta_1S_1P+F_1F_2F_5\beta_1\frac{\Lambda_1}{m_1}P-F_2F_5(m_1+\zeta_1)L_1\\
&-F_5\frac{(m_1+\zeta_1)}{\zeta_1}m_1I_1-F_3F_4F_5\frac{m_1k_2\zeta_2(m_1+\zeta_1)}{S_2k_1\zeta_1(m_2+\zeta_2)}\left(S_2-\frac{\Lambda_2}{m_2}\right)^2\\
&-F_3F_4F_5\frac{k_2m_1\zeta_2(m_1+\zeta_1)}{k_1m_2\zeta_1(m_2+\zeta_2)}\beta_2S_2P+F_3F_4F_5\frac{k_2m_1\zeta_2(m_1+\zeta_1)}{k_1m_2^2\zeta_1(m_2+\zeta_2)}\beta_2\Lambda_2P\\
&-F_4F_5\frac{k_2m_1\zeta_2(m_1+\zeta_1)}{k_1m_2\zeta_1}L_2-F_5\frac{k_2m_1(m_1+\zeta_1)}{k_1m_2\zeta_1}m_2I_2-\frac{m_1(m_1+\zeta_1)}{k_1\zeta_1}mP\\
&+F_1F_2F_5\beta_1S_1P+F_2F_5(m_1+\zeta_1)L_1+F_3F_4F_5\frac{k_2m_1\zeta_2(m_1+\zeta_1)}{k_1m_2\zeta_1(m_2+\zeta_2)}\beta_2S_2P\\
&+F_4F_5\frac{k_2m_1\zeta_2(m_1+\zeta_1)}{k_1m_2\zeta_1}L_2+F_5\frac{m_1(m_1+\zeta_1)}{k_1\zeta_1}\big[k_1I_1+k_2I_2\big].\end{aligned}$$

We collect terms as follows:

$$\begin{aligned}\frac{d\mathscr{F}_0^d}{dt} &= -F_1F_2F_5\frac{m_1}{S_1}\left(S_1-\frac{\Lambda_1}{m_1}\right)^2-F_3F_4F_5\frac{k_2m_1\zeta_2(m_1+\zeta_1)}{S_2k_1\zeta_1(m_2+\zeta_2)}\left(S_2-\frac{\Lambda_2}{m_2}\right)^2\\
&+\frac{mm_1(m_1+\zeta_1)}{k_1\zeta_1}\left(\frac{k_1\zeta_1\beta_1F_1F_2F_5\Lambda_1}{mm_1^2(m_1+\zeta_1)}+\frac{k_2\zeta_2\beta_2F_3F_4F_5\Lambda_2}{mm_2^2(m_2+\zeta_2)}-1\right)P.\end{aligned}$$

Finally, we obtain the following:

$$\begin{aligned}\frac{d\mathscr{F}_0^d}{dt} &= -F_1F_2F_5\frac{m_1}{S_1}\left(S_1-\frac{\Lambda_1}{m_1}\right)^2-F_3F_4F_5\frac{k_2m_1\zeta_2(m_1+\zeta_1)}{S_2k_1\zeta_1(m_2+\zeta_2)}\left(S_2-\frac{\Lambda_2}{m_2}\right)^2\\ &\quad+\frac{mm_1(m_1+\zeta_1)}{k_1\zeta_1}\left(\mathscr{R}_0^d-1\right)P.\end{aligned}$$

Therefore, for all $S_1,L_1,I_1,S_2,L_2,I_2,P>0$, we have $\frac{d\mathscr{F}_0^d}{dt}\leq 0$ when $\mathscr{R}_0^d\leq 1$. Moreover, $\frac{d\mathscr{F}_0^d}{dt}=0$ when $S_1=\frac{\Lambda_1}{m_1}$, $S_2=\frac{\Lambda_2}{m_2}$, and $(\mathscr{R}_0^d-1)P=0$. According to [19], solutions of system (2.1) limit to the largest invariant subset of $\left\{(S_1,L_1,I_1,S_2,L_2,I_2,P):\frac{d\mathscr{F}_0^d}{dt}=0\right\}$, which contains elements with $S_1(t)=\frac{\Lambda_1}{m_1}$, $S_2(t)=\frac{\Lambda_2}{m_2}$, and

$$(\mathscr{R}_0^d-1)P=0. \tag{4.2}$$

Let us consider two cases:

- If $\mathscr{R}_0^d<1$, then, we obtain $P=0$ from Eq (4.2). Since the largest invariant subset of $\left\{(S_1,L_1,I_1,S_2,L_2,I_2,P):\frac{d\mathscr{F}_0^d}{dt}=0\right\}$ is invariant, we obtain $\dot{P}(t)=0$. Then,

$$0=\int_0^{\omega_5}\zeta_5(\tau)e^{-\eta_5\tau}\left[k_1I_1(t-\tau)+k_2I_2(t-\tau)\right]d\tau\Rightarrow I_1(t)=I_2(t)=0,\forall t. \tag{4.3}$$

  Furthermore, since $I_1=0$, then $\dot{I}_2(t)=\zeta_1\int_0^{\omega_2}\zeta_2(\tau)e^{-\eta_2\tau}L_1(t-\tau)d\tau=0$, and thus $L_1(t)=0$, for any t. By the same way, $I_2=0$, then $\dot{I}_2(t)=\zeta_2\int_0^{\omega_4}\zeta_4(\tau)e^{-\eta_4\tau}L_2(t-\tau)d\tau=0$, and thus $L_2(t)=0$, for any t. Hence, the largest invariant subset of $\left\{(S_1,L_1,I_1,S_2,L_2,I_2,P):\frac{d\mathscr{F}_0^d}{dt}=0\right\}=\left\{\mathscr{E}_0^d\right\}$.

- If $\mathscr{R}_0^d=1$, then we have $S_1=\frac{\Lambda_1}{m_1}$, $S_2=\frac{\Lambda_2}{m_2}$; then, $\dot{S}_1(t)=\dot{S}_2(t)=0$. From (2.1), we have the following:

$$\Lambda_2-\Lambda_2-\beta_2\frac{\Lambda_2}{m_2}P=0\Longrightarrow P(t)=0,\forall t. \tag{4.4}$$

  According to (4.3), we deduce that $I_1(t)=I_2(t)=L_1(t)=L_2(t)=0$ for all $t\geq 0$. Hence, the largest invariant subset of $\left\{(S_1,L_1,I_1,S_2,L_2,I_2,P):\frac{d\mathscr{F}_0^d}{dt}=0\right\}=\left\{\mathscr{E}_0^d\right\}$.

By applying LaSalle's invariance principle [26], we conclude that $\mathscr{E}_0^d=\left(\frac{\Lambda_1}{m_1},0,0,\frac{\Lambda_2}{m_2},0,0,0\right)$ is globally asymptotically stable once $\mathscr{R}_0^d\leq 1$. □

Theorem 5. *If the dual target-infection equilibrium point $\mathscr{E}_d^*$ exists ($\mathscr{R}_0^d > 1$), then it is globally asymptotically stable.*

This theorem establishes the global attractiveness of the endemic equilibrium in the delayed model, thereby generalizing Theorem 3. It confirms that the threshold dynamics are preserved: when $\mathscr{R}_0^d > 1$, the disease will persist at an endemic level for all initial histories, and the inclusion of delays does not induce sustained oscillations or other complex behaviors that could invalidate the simple dichotomy.

Proof. Let us define a candidate Lyapunov function $\mathscr{F}_d^*(S_1, L_1, I_1, S_2, L_2, I_2, P)$ as follows:

$$\begin{aligned}
\mathscr{F}_d^* &= F_1F_2F_5S_1^*\Phi\left(\frac{S_1}{S_1^*}\right) + F_2F_5L_1^*\Phi\left(\frac{L_1}{L_1^*}\right) + F_5\frac{m_1+\zeta_1}{\zeta_1}I_1^*\Phi\left(\frac{I_1}{I_1^*}\right)\\
&\quad + F_3F_4F_5\frac{k_2m_1\zeta_2(m_1+\zeta_1)}{k_1m_2\zeta_1(m_2+\zeta_2)}S_2^*\Phi\left(\frac{S_2}{S_2^*}\right) + F_4F_5\frac{k_2m_1\zeta_2(m_1+\zeta_1)}{k_1m_2\zeta_1(m_2+\zeta_2)}L_2^*\Phi\left(\frac{L_2}{L_2^*}\right)\\
&\quad + F_5\frac{k_2m_1(m_1+\zeta_1)}{k_1m_2\zeta_1}I_2^*\Phi\left(\frac{I_2}{I_2^*}\right) + \frac{m_1(m_1+\zeta_1)}{k_1\zeta_1}P^*\Phi\left(\frac{P}{P^*}\right)\\
&\quad + F_2F_5\beta_1S_1^*P^*\int_0^{\omega_1}G_1(\tau)\int_{t-\tau}^{t}\Phi\left(\frac{S_1(\theta)P(\theta)}{S_1^*P^*}\right)d\theta d\tau\\
&\quad + F_5(m_1+\zeta_1)L_1^*\int_0^{\omega_2}G_2(\tau)\int_{t-\tau}^{t}\Phi\left(\frac{L_1(\theta)}{L_1^*}\right)d\theta d\tau\\
&\quad + F_4F_5\beta_2\frac{k_2m_1\zeta_2(m_1+\zeta_1)}{k_1m_2\zeta_1(m_2+\zeta_2)}S_2^*P^*\int_0^{\omega_3}G_3(\tau)\int_{t-\tau}^{t}\Phi\left(\frac{S_2(\theta)P(\theta)}{S_2^*P^*}\right)d\theta d\tau\\
&\quad + F_5\frac{k_2m_1\zeta_2(m_1+\zeta_1)}{k_1m_2\zeta_1}L_2^*\int_0^{\omega_4}G_4(\tau)\int_{t-\tau}^{t}\Phi\left(\frac{L_2(\theta)}{L_2^*}\right)d\theta d\tau\\
&\quad + \frac{m_1(m_1+\zeta_1)}{k_1\zeta_1}\int_0^{\omega_5}G_5(\tau)\int_{t-\tau}^{t}\left(k_1I_1^*\Phi\left(\frac{I_1(\theta)}{I_1^*}\right) + k_2I_2^*\Phi\left(\frac{I_2(\theta)}{I_2^*}\right)\right)d\theta d\tau.
\end{aligned}$$

The Lyapunov functional $\mathscr{F}_d^*$ is defined on the biologically feasible set Σ^d. It maps states in Σ^d to nonnegative real numbers, is smooth on the interior of Σ^d, and only equals to zero at the disease-free equilibrium $\mathscr{E}_d^*$.

By calculating $\dfrac{d\mathscr{F}_d^*}{dt}$ along the trajectories of dynamics (2.1), we obtain the following:

$$\begin{aligned}
\frac{d\mathscr{F}_d^*}{dt} &= F_1F_2F_5\left(1-\frac{S_1^*}{S_1}\right)(\Lambda_1 - m_1S_1 - \beta_1S_1P)\\
&\quad + F_2F_5\left(1-\frac{L_1^*}{L_1}\right)\left(\beta_1\int_0^{\omega_1}G_1S_1^\tau P^\tau d\tau - (m_1+\zeta_1)L_1\right)\\
&\quad + F_5\frac{m_1+\zeta_1}{\zeta_1}\left(1-\frac{I_1^*}{I_1}\right)\left(\zeta_1\int_0^{\omega_2}G_2L_1^\tau d\tau - m_1I_1\right)\\
&\quad + F_3F_4F_5\frac{k_2m_1\zeta_2(m_1+\zeta_1)}{k_1m_2\zeta_1(m_2+\zeta_2)}\left(1-\frac{S_2^*}{S_2}\right)(\Lambda_2 - m_2S_2 - \beta_2S_2P)\\
&\quad + F_4F_5\frac{k_2m_1\zeta_2(m_1+\zeta_1)}{k_1m_2\zeta_1(m_2+\zeta_2)}\left(1-\frac{L_2^*}{L_2}\right)\left(\beta_2\int_0^{\omega_3}G_3S_2^\tau P^\tau d\tau - (m_2+\zeta_2)L_2\right)\\
&\quad + F_5\frac{k_2m_1(m_1+\zeta_1)}{k_1m_2\zeta_1}\left(1-\frac{I_2^*}{I_2}\right)\left(\zeta_2\int_0^{\omega_4}G_4L_2^\tau d\tau - m_2I_2\right)
\end{aligned}$$

$$
\begin{aligned}
&+\frac{m_1(m_1+\zeta_1)}{k_1\zeta_1}\left(1-\frac{P^*}{P}\right)\left(\int_0^{\omega_5} G_5\left[k_1I_1^\tau+k_2I_2^\tau\right]d\tau-mP\right)\\
&+F_2F_5\beta_1S_1^*P^*\int_0^{\omega_1} G_1(\tau)\left[\frac{S_1P}{S_1^*P^*}-\frac{S_1^\tau P^\tau}{S_1^*P^*}+\ln\left(\frac{S_1^\tau P^\tau}{S_1P}\right)\right]d\tau\\
&+F_5(m_1+\zeta_1)L_1^*\int_0^{\omega_2} G_2(\tau)\left[\frac{L_1}{L_1^*}-\frac{L_1^\tau}{L_1^*}+\ln\left(\frac{L_1^\tau}{L_1}\right)\right]d\tau\\
&+F_4F_5\beta_2\frac{k_2m_1\zeta_2(m_1+\zeta_1)}{k_1m_2\zeta_1(m_2+\zeta_2)}S_2^*P^*\int_0^{\omega_3} G_3(\tau)\left[\frac{S_2P}{S_2^*P^*}-\frac{S_2^\tau P^\tau}{S_2^*P^*}+\ln\left(\frac{S_2^\tau P^\tau}{S_2P}\right)\right]d\tau\\
&+F_5\frac{k_2m_1\zeta_2(m_1+\zeta_1)}{k_1m_2\zeta_1}L_2^*\int_0^{\omega_4} G_4(\tau)\left[\frac{L_2}{L_2^*}-\frac{L_2^\tau}{L_2^*}+\ln\left(\frac{L_2^\tau}{L_2}\right)\right]d\tau\\
&+\frac{m_1(m_1+\zeta_1)}{k_1\zeta_1}\int_0^{\omega_5} G_5(\tau)\left(k_1I_1^*\left[\frac{I_1}{I_1^*}-\frac{I_1^\tau}{I_1^*}+\ln\left(\frac{I_1^\tau}{I_1}\right)\right]+k_2I_2^*\left[\frac{I_2}{I_2^*}-\frac{I_2^\tau}{I_2^*}+\ln\left(\frac{I_2^\tau}{I_2}\right)\right]\right)d\tau.
\end{aligned}
$$

By using the equilibrium conditions

$$
\begin{aligned}
&\Lambda_1=m_1S_1^*+\beta_1S_1^*P^*,\ \Lambda_2=m_2S_2^*+\beta_2S_2^*P^*,\ F_5(k_1I_1^*+k_2I_2^*)=mP^*,\\
&\beta_1F_1S_1^*P^*=(m_1+\zeta_1)L_1^*,\zeta_1F_2L_1^*=m_1I_1^*,\ \beta_2F_3S_2^*P^*=(m_2+\zeta_2)L_2^*,\zeta_2F_4L_2^*=m_2I_2^*,
\end{aligned}
$$

we get $m_1I_1^*=\zeta_1F_2L_1^*=\dfrac{\zeta_1F_1F_2}{(m_1+\zeta_1)}\beta_1S_1^*P^*, m_2I_2^*=\zeta_2F_4L_2^*=\dfrac{\zeta_2F_3F_4}{(m_2+\zeta_2)}\beta_2S_2^*P^*,$ and

$$
\begin{aligned}
\frac{d\mathscr{F}_d^*}{dt} &= -F_1F_2F_5\frac{m_1(S_1-S_1^*)^2}{S_1}-F_3F_4F_5\frac{k_2m_1\zeta_2(m_1+\zeta_1)}{k_1m_2\zeta_1(m_2+\zeta_2)}\frac{m_2(S_2-S_2^*)^2}{S_2}\\
&\quad+F_1F_2F_5\beta_1S_1^*P^*\left(1-\frac{S_1^*}{S_1}\right)+F_3F_4F_5\frac{k_2m_1\zeta_2(m_1+\zeta_1)}{k_1m_2\zeta_1(m_2+\zeta_2)}\beta_2S_2^*P^*\left(1-\frac{S_2^*}{S_2}\right)\\
&\quad+F_2F_5\beta_1S_1^*P^*\int_0^{\omega_1} G_1(\tau)\left[1-\frac{S_1^\tau P^\tau L_1^*}{S_1^*P^*L_1}+\ln\left(\frac{S_1^\tau P^\tau}{S_1P}\right)\right]d\tau\\
&\quad+F_1F_5\beta_1S_1^*P^*\int_0^{\omega_2} G_2(\tau)\left[1-\frac{L_1^\tau I_1^*}{L_1^*I_1}+\ln\left(\frac{L_1^\tau}{L_1}\right)\right]d\tau\\
&\quad+F_4F_5\frac{k_2m_1\zeta_2(m_1+\zeta_1)}{k_1m_2\zeta_1(m_2+\zeta_2)}\beta_2S_2^*P^*\int_0^{\omega_3} G_3(\tau)\left[1-\frac{S_2^\tau P^\tau L_2^*}{S_2^*P^*L_2}+\ln\left(\frac{S_2^\tau P^\tau}{S_2P}\right)\right]d\tau\\
&\quad+F_3F_5\frac{k_2m_1\zeta_2(m_1+\zeta_1)}{k_1m_2\zeta_1(m_2+\zeta_2)}\beta_2S_2^*P^*\int_0^{\omega_4} G_4(\tau)\left[1-\frac{L_2^\tau I_2^*}{L_2^*I_2}+\ln\left(\frac{L_2^\tau}{L_2}\right)\right]d\tau\\
&\quad+F_1F_2\beta_1S_1^*P^*\int_0^{\omega_5} G_5(\tau)\left[1-\frac{I_1^\tau P^*}{I_1^*P}+\ln\left(\frac{I_1^\tau}{I_1}\right)\right]d\tau\\
&\quad+F_3F_4\frac{k_2m_1\zeta_2(m_1+\zeta_1)}{k_1m_2\zeta_1(m_2+\zeta_2)}\beta_2S_2^*P^*\int_0^{\omega_5} G_5(\tau)\left[1-\frac{I_2^\tau P^*}{I_2^*P}+\ln\left(\frac{I_2^\tau}{I_2}\right)\right]d\tau.
\end{aligned}
$$

By applying the equalities:

$$
\begin{aligned}
&\ln\left(\frac{S_1^\tau P^\tau}{S_1P}\right)+\ln\left(\frac{L_1^\tau}{L_1}\right)+\ln\left(\frac{I_1^\tau}{I_1}\right)=\ln\left(\frac{S_1^*}{S_1}\right)+\ln\left(\frac{S_1^\tau P^\tau L_1^*}{S_1^*P^*L_1}\right)+\ln\left(\frac{L_1^\tau I_1^*}{L_1^*I_1}\right)+\ln\left(\frac{I_1^\tau P^*}{I_1^*P}\right),\\
&\ln\left(\frac{S_2^\tau P^\tau}{S_2P}\right)+\ln\left(\frac{L_2^\tau}{L_2}\right)+\ln\left(\frac{I_2^\tau}{I_2}\right)=\ln\left(\frac{S_2^*}{S_2}\right)+\ln\left(\frac{S_2^\tau P^\tau L_2^*}{S_2^*P^*L_2}\right)+\ln\left(\frac{L_2^\tau I_2^*}{L_2^*I_2}\right)+\ln\left(\frac{I_2^\tau P^*}{I_2^*P}\right),
\end{aligned}
$$

we obtain the following:

$$\begin{aligned}
\frac{d\mathscr{F}_d^*}{dt} &= -F_1F_2F_5\frac{m_1(S_1-S_1^*)^2}{S_1} - F_3F_4F_5\frac{k_2m_1\zeta_2(m_1+\zeta_1)}{k_1m_2\zeta_1(m_2+\zeta_2)}\frac{m_2(S_2-S_2^*)^2}{S_2} \\
&\quad -F_1F_2F_5\beta_1S_1^*P^*\Phi\left(\frac{S_1^*}{S_1}\right) - F_3F_4F_5\frac{k_2m_1\zeta_2(m_1+\zeta_1)}{k_1m_2\zeta_1(m_2+\zeta_2)}\beta_2S_2^*P^*\Phi\left(\frac{S_2^*}{S_2}\right) \\
&\quad -F_2F_5\beta_1S_1^*P^*\int_0^{\omega_1}G_1(\tau)\Phi\left(\frac{S_1^\tau P^\tau}{S_1^*P^*}\frac{L_1^*}{L_1}\right)d\tau - F_1F_5\beta_1S_1^*P^*\int_0^{\omega_2}G_2(\tau)\Phi\left(\frac{I_1^*}{I_1}\frac{L_1^\tau}{L_1^*}\right)d\tau \\
&\quad -F_4F_5\frac{k_2m_1\zeta_2(m_1+\zeta_1)}{k_1m_2\zeta_1(m_2+\zeta_2)}\beta_2S_2^*P^*\int_0^{\omega_3}G_3(\tau)\Phi\left(\frac{S_2^\tau P^\tau}{S_2^*P^*}\frac{L_2^*}{L_2}\right)d\tau \\
&\quad -F_3F_5\frac{k_2m_1\zeta_2(m_1+\zeta_1)}{k_1m_2\zeta_1(m_2+\zeta_2)}\beta_2S_2^*P^*\int_0^{\omega_4}G_4(\tau)\Phi\left(\frac{L_2^\tau}{L_2^*}\frac{I_2^*}{I_2}\right)d\tau \\
&\quad -F_1F_2\beta_1S_1^*P^*\int_0^{\omega_5}G_5(\tau)\Phi\left(\frac{I_1^\tau}{I_1^*}\frac{P^*}{P}\right)d\tau \\
&\quad -F_3F_4\frac{k_2m_1\zeta_2(m_1+\zeta_1)}{k_1m_2\zeta_1(m_2+\zeta_2)}\beta_2S_2^*P^*\int_0^{\omega_5}G_5(\tau)\Phi\left(\frac{I_2^\tau}{I_2^*}\frac{P^*}{P}\right)d\tau.
\end{aligned}$$

Therefore, $\frac{d\mathscr{F}_d^*}{dt} \leq 0$. Furthermore, $\frac{d\mathscr{F}_d^*}{dt} = 0$ exactly if $(S_1,L_1,I_1,S_2,L_2,I_2,P) = (S_1^*,L_1^*,I_1^*,S_2^*,L_2^*,I_2^*,P^*)$. By using LaSalle's invariance principle, we deduce that $\mathscr{E}_d^*$ is globally asymptotically stable once $\mathscr{R}_0^d > 1$. □

The analytical results of this section provide the framework for the delayed system. In Section 5, numerical simulations will be used to validate these stability results and to investigate the quantitative impact of the distributed delays on the infection dynamics.

5. Numerical simulations

In this section, we complement the theoretical results obtained in the previous analyses with a comprehensive set of numerical simulations. These experiments aim to validate the analytical findings regarding the global stability of equilibria and to illustrate the dynamic behavior of the system under various biological and epidemiological scenarios. By exploring different parameter regimes, we examine how variations in the transmission rates, latency periods, and treatment efficacies influence the progression and control of dual Nosema infections in interacting honeybee colonies. Furthermore, a sensitivity analysis is performed to identify the key parameters that most significantly affect the delayed basic reproduction number $\mathscr{R}_0^d$, thus providing valuable insights into effective intervention strategies. The numerical results not only confirm the theoretical predictions but also offer practical guidance to optimize the treatment protocols and manage the disease persistence within multi-colony apiaries.

The numerical simulations are performed using a discrete-delay formulation derived from the general distributed-delay model by choosing a specific probability density function, namely the Dirac delta $\delta(\cdot)$. This choice effectively reduces the integral terms to discrete delayed variables [27, 28], which are computationally easier to handle with standard Delay Differential Equations (DDE) solvers such as MATLAB's dde23. Below, we explain the mathematical justification for this reduction and why it is a legitimate approximation for numerical purposes.

The original distributed-delay model (system (2.1)) contains terms of the following form: $\int_0^{\omega_i} G_i(\tau)Z(t-\tau)\,d\tau$, where $G_i(\tau) = q_i(\tau)e^{-\eta_i\tau}$, and $q_i(\tau)$ is a probability density function. If we select $q_i(\tau) = \delta(\tau-\tau_i)$, then

$$\int_0^{\infty} \delta(\tau-\tau_i)e^{-\eta_i\tau}Z(t-\tau)\,d\tau = e^{-\eta_i\tau_i}Z(t-\tau_i) = e^{-\eta_i\tau_i}Z^{\tau_i}.$$

Thus, the distributed delay is replaced by a single discrete delay τ_i multiplied by a survival factor $e^{-\eta_i\tau_i}$. This is a standard simplification in DDEs when the delay distribution is highly concentrated around a mean value. This approach is used for simulations since the following hold:

1. Discrete-delay systems are directly solvable with widely available numerical DDE solvers;
2. the Dirac delta represents the case where the delay is fixed (non-distributed), which is a common first approximation when detailed distributions are unknown; and
3. the discrete-delay version retains the essential dynamic features analyzed in the paper (threshold R_0^d, stability switches, etc.), while allowing explicit computation of trajectories.

Hence, the dynamics (2.1) will be written as follows:

$$\begin{cases} \dot{S}_1 &= \Lambda_1 - m_1S_1 - \beta_1S_1P, \\ \dot{L}_1 &= \beta_1e^{-\eta_1\tau_1}S_1^{\tau_1}P^{\tau_1} - (m_1+\zeta_1)L_1, \\ \dot{I}_1 &= \zeta_1e^{-\eta_2\tau_2}L_1^{\tau_2} - m_1I_1, \\ \dot{S}_2 &= \Lambda_2 - m_2S_2 - \beta_2S_2P, \\ \dot{L}_2 &= \beta_2e^{-\eta_3\tau_3}S_2^{\tau_3}P^{\tau_3} - (m_2+\zeta_2)L_2, \\ \dot{I}_2 &= \zeta_2e^{-\eta_4\tau_4}L_2^{\tau_4} - m_2I_2, \\ \dot{P} &= e^{-\eta_5\tau_5}\left[k_1I_1^{\tau_5} + k_2I_2^{\tau_5}\right] - mP. \end{cases} \tag{5.1}$$

The basic reproduction number of model (5.1) is provided hereafter as follows:

$$\mathscr{R}_0^d = \frac{k_1\zeta_1\beta_1\Lambda_1}{mm_1^2(m_1+\zeta_1)}e^{-(\eta_1\tau_1+\eta_2\tau_2+\eta_5\tau_5)} + \frac{k_2\zeta_2\beta_2\Lambda_2}{mm_2^2(m_2+\zeta_2)}e^{-(\eta_3\tau_3+\eta_4\tau_4+\eta_5\tau_5)}.$$

The parameter values listed in Table 2 are employed for the numerical simulations. We allow for colony-specific parameters to account for the heterogeneity commonly observed in apiaries, where colonies differ in size, genetic resistance, and management, thus enabling the study of cross-colony spillover dynamics. The initial value problem is solved using MATLAB's ode45 solver to numerically integrate the system and verify the theoretical findings presented in the previous sections. To examine the influence of key parameters on the threshold quantities and stability behavior, selected values are systematically varied. Furthermore, the system of delay differential equations (5.1) is numerically solved using MATLAB's dde23 solver. For simplicity, we assume $\eta_i = 1$ and set the delay parameters to $\tau_i = 0.1$ for $i = 1,\cdots,5$

Table 2. Parameter values that are chosen arbitrarily and without biological significance.

Parameter	Λ_1	Λ_2	ζ_1	ζ_2	m_1	m_2	k_1	k_2	m	
Value	20	30	0.01	0.05	0.02	0.03	0.01	0.009	0.4	
Parameter	τ_1	τ_2	τ_3	τ_4	τ_5	η_1	η_2	η_3	η_4	η_5
Value	0.1	0.1	0.1	0.1	0.1	1	1	1	1	1

5.1. Stability of equilibria

By varying the initial condition, we validate the theoretical findings derived in Section 4. For two different set of infection rates β_1 and β_2, we obtain the following two cases:

- For $\beta_1 = 0.0003$ and $\beta_2 = 0.00002$, we obtain $\mathscr{R}_0^d = 0.1019 < 1$.
  The trajectories of dynamics (2.1) converge to the infection-free equilibrium point $\mathscr{E}_0^d = (1000, 0, 0, 1000, 0, 0, 0)$ (Figure 2), thus confirming the results provided in Theorems 2 and 4, where the trajectories of dynamics (2.1) converge to $\mathscr{E}_0^d$.
- For $\beta_1 = 0.02$ and $\beta_2 = 0.03$, we obtain $\mathscr{R}_0^d = 16.5912 > 1$.
  The trajectories of dynamics (2.1) converge to the endemic equilibrium point $\mathscr{E}_d^* = (60.26, 566.87, 256.55, 60.26, 318.86, 480.87, 15.59)$ (Figure 3), thus confirming the theoretical results provided in Theorems 3 and 5.

Figure 2 illustrates the case where the delayed basic reproduction number satisfies $\mathscr{R}_0^d < 1$. Under this condition, the infection cannot sustain itself in the long term. Biologically, this means that the average number of secondary infections produced by a single infected bee is insufficient to replace itself, thus leading to the eventual extinction of the pathogen. The trajectories show the following:

- The latent and infectious bee populations in both colonies (L_1, I_1, L_2, I_2) decline to zero;
- the environmental spore load $P(t)$ also decays to zero, indicating no persistent contamination; and
- the healthy bee populations S_1 and S_2 recover and stabilize at their carrying capacities $\frac{\Lambda_1}{m_1}$ and $\frac{\Lambda_2}{m_2}$, respectively.

This scenario reflects successful disease containment, possibly due to low transmission rates, high bee mortality, effective treatment, or prolonged pathogen maturation delays that reduce $\mathscr{R}_0^d$ below the critical threshold.

Figure 3 depicts the endemic state where $\mathscr{R}_0^d > 1$. Here, the infection establishes itself in both colonies and persists at a stable positive level. Biologically, this indicates that the pathogen is able to maintain continuous transmission through the shared environment. The model predicts the following:

- The susceptible bee populations S_1 and S_2 settle at reduced levels compared to the disease-free state;
- Latent (L_1, L_2) and infectious (I_1, I_2) compartments stabilize at positive values, thus reflecting ongoing infection cycles; and
- The environmental spore concentration $P(t)$ remains positive, thus confirming a contaminated environment that facilitates indirect transmission.

This endemic equilibrium illustrates how a single infected colony can act as a reservoir, thereby spreading Nosema spores via the environment and leading to sustained infections in both hives. Such a situation may arise from high transmission rates, efficient spore shedding, or an insufficient natural decay of spores in the environment—factors that collectively raise $\mathscr{R}_0^d$ above 1.

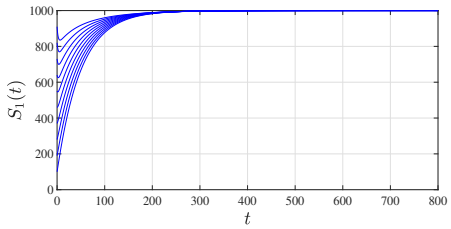

(a) Uninfected bees from colony 1.

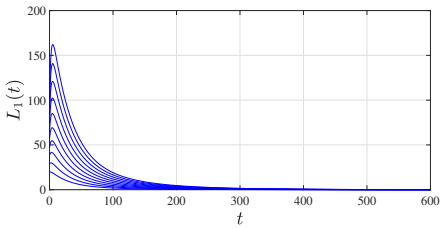

(b) Latent infected bees from colony 1.

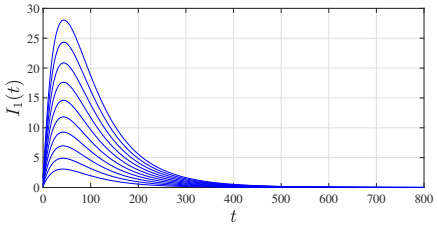

(c) Active infected bees from colony 1.

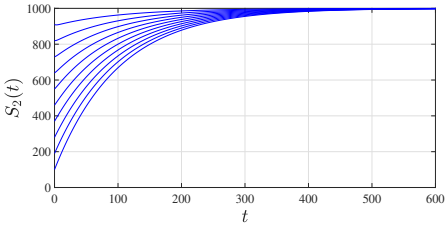

(d) Uninfected bees from colony 2.

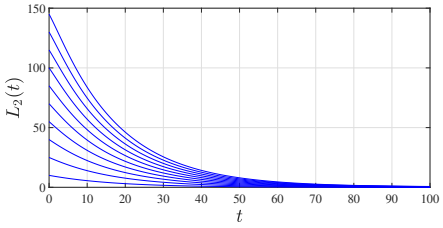

(e) Latent infected bees from colony 2.

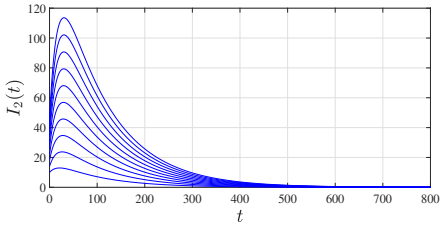

(f) Active infected bees from colony 2.

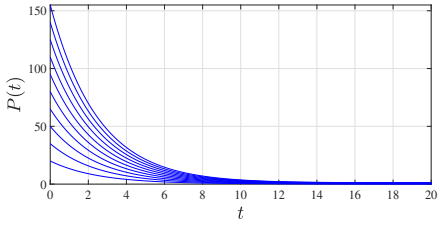

(g) Virus.

Figure 2. Dynamics of the dual-colony Nosema infection model when $\mathscr{R}_0^d < 1$. All infected compartments (L_1, I_1, L_2, I_2) and environmental spores (P) converge to zero, while susceptible bee populations (S_1, S_2) stabilize at their disease-free equilibrium levels.

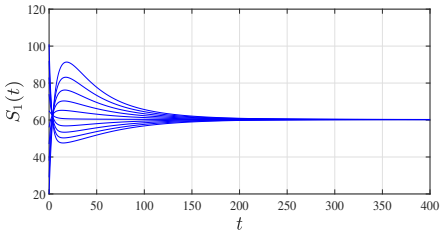

(a) Uninfected bees from colony 1.

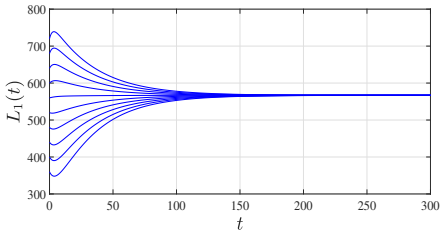

(b) Latent infected bees from colony 1.

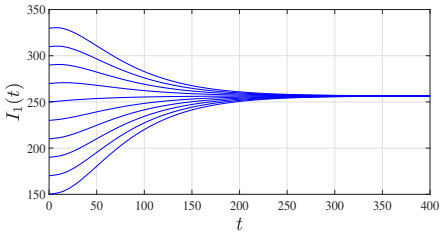

(c) Active infected bees from colony 1.

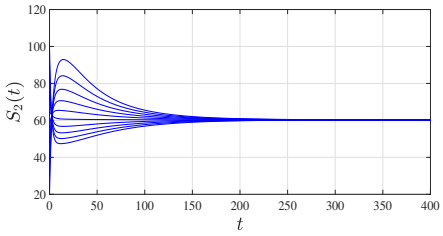

(d) Uninfected bees from colony 2.

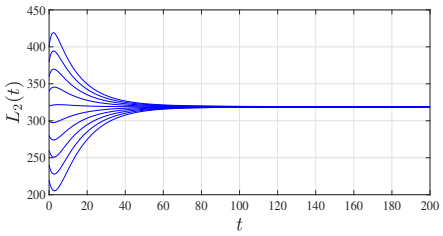

(e) Latent infected bees from colony 2.

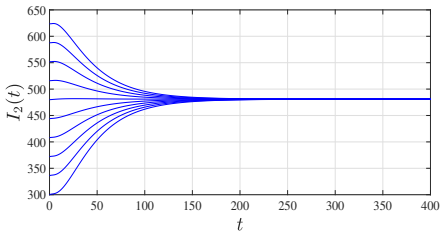

(f) Active infected bees from colony 2.

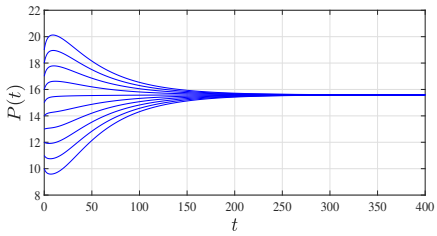

(g) Virus.

Figure 3. Dynamics of the dual-colony Nosema infection model when $\mathscr{R}_0^d > 1$. The system converges to an endemic equilibrium where infection persists in both colonies and the environment.

5.2. Sensitivity analysis

A sensitivity analysis aims to assess and quantify how variations in the input parameters affect the output of a mathematical model [22]. This is commonly done through the use of sensitivity indices, which express the relative change in a model outcome that results from a proportional change in a given parameter. Such an approach enables the identification of parameters that exert the strongest influence on the basic reproduction number, $\mathscr{R}_0^d$. Because $\mathscr{R}_0^d$ is differentiable with respect to several model parameters, these indices can be analytically computed using partial derivatives [29]. The purpose of

this analysis is to examine how variations in the model's parameters affect $\mathscr{R}_0^d$ and, consequently, the stability of the infection-free equilibrium $\mathscr{E}_0^d$. The sensitivity index of $\mathscr{R}_0^d$ with respect to a parameter ν is defined as follows [22]:

$$S_\nu^{\mathscr{R}_0^d} = \frac{\partial \mathscr{R}_0^d}{\partial \nu} \times \frac{\nu}{\mathscr{R}_0^d}.$$

$\mathscr{R}_0^d$ is given by $\mathscr{R}_0^d = \dfrac{\zeta_1 k_1 \beta_1 \Lambda_1}{m m_1^2 (m_1+\zeta_1)} e^{-(\eta_1\tau_1+\eta_2\tau_2+\eta_5\tau_5)} + \dfrac{\zeta_2 k_2 \beta_2 \Lambda_2}{m m_2^2 (m_2+\zeta_2)} e^{-(\eta_3\tau_3+\eta_4\tau_4+\eta_5\tau_5)}$. Therefore, we obtain the following:

$$\begin{aligned}
S_{\Lambda_1}^{\mathscr{R}_0^d} &= S_{k_1}^{\mathscr{R}_0^d} = S_{\beta_1}^{\mathscr{R}_0^d} = \frac{\zeta_1 k_1 \beta_1 \Lambda_1}{m m_1^2 \mathscr{R}_0^d (m_1+\zeta_1)} e^{-(\eta_1\tau_1+\eta_2\tau_2+\eta_5\tau_5)},\\
S_{\Lambda_2}^{\mathscr{R}_0^d} &= S_{k_2}^{\mathscr{R}_0^d} = S_{\beta_2}^{\mathscr{R}_0^d} = \frac{\zeta_2 k_2 \beta_2 \Lambda_2}{m m_2^2 \mathscr{R}_0 (m_2+\zeta_2)} e^{-(\eta_3\tau_3+\eta_4\tau_4+\eta_5\tau_5)},\\
S_{\eta_1}^{\mathscr{R}_0^d} &= S_{\tau_1}^{\mathscr{R}_0^d} = -\frac{\eta_1\tau_1\zeta_1 k_1 \beta_1 \Lambda_1}{m m_1^2 (m_1+\zeta_1)\mathscr{R}_0} e^{-(\eta_1\tau_1+\eta_2\tau_2+\eta_5\tau_5)},\\
S_{\eta_2}^{\mathscr{R}_0} &= S_{\tau_2}^{\mathscr{R}_0^d} = -\frac{\eta_2\tau_2\zeta_1 k_1 \beta_1 \Lambda_1}{m m_1^2 (m_1+\zeta_1)\mathscr{R}_0^d} e^{-(\eta_1\tau_1+\eta_2\tau_2+\eta_5\tau_5)},\\
S_{\eta_3}^{\mathscr{R}_0^d} &= S_{\tau_3}^{\mathscr{R}_0^d} = -\frac{\eta_3\tau_3\zeta_2 k_2 \beta_2 \Lambda_2}{m m_2^2 (m_2+\zeta_2)\mathscr{R}_0} e^{-(\eta_3\tau_3+\eta_4\tau_4+\eta_5\tau_5)},\\
S_{\eta_4}^{\mathscr{R}_0^d} &= S_{\tau_4}^{\mathscr{R}_0^d} = -\frac{\eta_4\tau_4\zeta_2 k_2 \beta_2 \Lambda_2}{m m_2^2 (m_2+\zeta_2)\mathscr{R}_0^d} e^{-(\eta_3\tau_3+\eta_4\tau_4+\eta_5\tau_5)},\\
S_{m_1}^{\mathscr{R}_0^d} &= \frac{-\zeta_1 k_1 \beta_1 \Lambda_1 (2(m_1+\zeta_1)+m_1)}{\mathscr{R}_0^d m m_1^2 (m_1+\zeta_1)^2} e^{-(\eta_1\tau_1+\eta_2\tau_2+\eta_5\tau_5)},\\
S_{m_2}^{\mathscr{R}_0^d} &= \frac{-\zeta_2 k_2 \beta_2 \Lambda_2 (2(m_2+\zeta_2)+m_2)}{\mathscr{R}_0^d m m_2^2 (m_2+\zeta_2)^2} e^{-(\eta_3\tau_3+\eta_4\tau_4+\eta_5\tau_5)},\\
S_{\zeta_1}^{\mathscr{R}_0^d} &= \frac{\zeta_1 k_1 \beta_1 \Lambda_1}{\mathscr{R}_0^d m m_1 (m_1+\zeta_1)^2} e^{-(\eta_1\tau_1+\eta_2\tau_2+\eta_5\tau_5)},\\
S_{\zeta_2}^{\mathscr{R}_0^d} &= \frac{\zeta_2 k_2 \beta_2 \Lambda_2}{\mathscr{R}_0 m m_2 (m_2+\zeta_2)^2} e^{-(\eta_3\tau_3+\eta_4\tau_4+\eta_5\tau_5)},\\
S_{\eta_5}^{\mathscr{R}_0^d} &= S_{\tau_5}^{\mathscr{R}_0^d} = -\eta_5\tau_5, S_m^{\mathscr{R}_0^d} = -1.
\end{aligned}$$

By choosing $\beta_1 = 0.02$ and $\beta_2 = 0.03$, the sensitivity indices of $\mathscr{R}_0^d$ are calculated in Table 3.

Table 3. Sensitivity of $\mathscr{R}_0^d$.

Parameter ν	Λ_1	k_1	β_1	Λ_2	k_2	β_2	ζ_1
$S_\nu^{\mathscr{R}_0^d}$	0.3721	0.3721	0.3721	0.6279	0.6279	0.6279	0.2481
Parameter ν	ζ_2	τ_1	η_1	τ_2	η_2	τ_3	η_3
$S_\nu^{\mathscr{R}_0^d}$	0.2355	-0.0372	-0.0372	-0.0372	-0.0372	-0.0628	-0.0628
Parameter ν	η_4	τ_4	η_5	τ_5	m_1	m_2	m
$S_\nu^{\mathscr{R}_0^d}$	-0.0628	-0.0628	-0.1	-0.1	-0.6202	-0.8634	-1

The sensitivity analysis quantifies the relative impact of each parameter on the basic reproduction number $\mathscr{R}_0^d$, which serves as a threshold to determine whether the dual Nosema infection persists or dies out in the honeybee colonies. Each sensitivity index $S_{\mathscr{R}_0^d}^{\nu}$ measures the proportional change in $\mathscr{R}_0^d$ that results from a proportional change in the parameter ν. According to Table 3, parameters associated with the *transmission process*, namely the transmission rates β_1 and β_2, the spore shedding rates k_1 and k_2, and the recruitment rates Λ_1 and Λ_2, exhibit the highest positive sensitivity indices. This implies that even small increases in these parameters substantially raise $\mathscr{R}_0^d$, thus enhancing the infection persistence within and between colonies. Biologically, a higher transmission efficiency or an increased spore release from infected bees intensifies the environmental contamination, thus accelerating disease spread. In contrast, parameters such as the natural death rates m_1 and m_2, and the environmental spore decay rate m, show negative sensitivity indices. An increase in these parameters leads to a reduction in $\mathscr{R}_0^d$, which indicates that an elevated mortality or faster pathogen degradation in the environment suppresses infection. This observation agrees with epidemiological expectations, as a greater removal or decay rates limit the availability of infectious agents and contribute to disease eradication. Figure 4 provides a visual ranking of the sensitivity indices, thereby highlighting the parameters that exert the greatest influence on $\mathscr{R}_0^d$. The tallest bars correspond to β_1, β_2, k_1, and k_2, thus confirming that inter-colony transmission and spore release are the dominant factors that govern infection dynamics. Parameters with negative bars represent control factors that mitigate infection when increased.

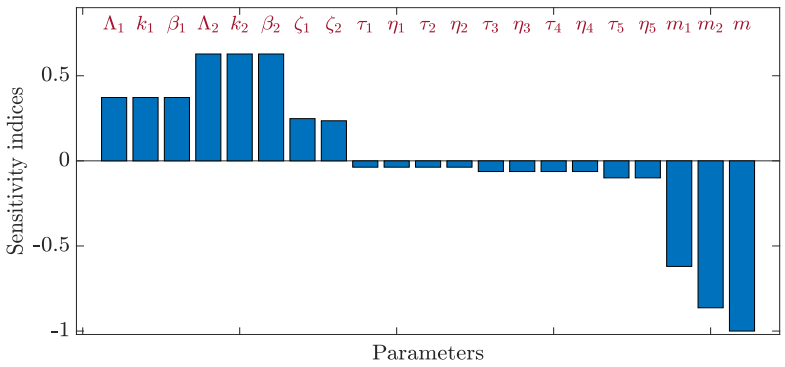

Figure 4. Sensitivity analysis.

From a biological standpoint, the sensitivity results suggest that effective management strategies

should focus on the following: (i) reducing transmission coefficients (β_i) through improved colony hygiene and reduced contact with contaminated resources; (ii) lowering spore shedding rates (k_i) via targeted treatment or disinfection; and (iii) enhancing natural or environmental clearance mechanisms by promoting hygienic bee behaviors or improving conditions that accelerate pathogen decay. Overall, the analysis demonstrates that $\mathscr{R}_0^d$ is most sensitive to transmission-related parameters, while natural mortality and decay act as stabilizing forces that favor disease control.

5.3. Influence of treatments on the dynamics

In this subsection, we examine the effects of antiviral treatment interventions on the dynamics of the dual Nosema infection model. The inclusion of the treatment allows us to quantitatively assess how reductions in the transmission and shedding rates influence the basic reproduction number $\mathscr{R}_0^d$ and the long-term behavior of the system. Through numerical simulations, we explore different levels of treatment efficacy to identify threshold values that ensure infection eradication or persistence. This analysis provides important insights into the potential effectiveness of pharmacological and management-based control strategies in mitigating the spread of Nosema disease within and across honeybee colonies.

To model the effect of an antiviral or antimicrobial treatment, we introduce an efficacy parameter $\kappa \in [0,1]$. We assume the treatment acts by reducing the probability that contact with an environmental spore leads to a successful infection. This is modeled by scaling the transmission coefficients β_1 and β_2 by the factor $(1-\kappa)$. This formulation implicitly assumes that the treatment:

- Does not cure already infected bees (latent or active),
- does not reduce the spore-shedding rate of infectious bees,
- does not alter the natural mortality rates or the pathogen's incubation period, and
- does not directly degrade spores in the environment.

This is a simplified representation of a prophylactic or transmission-blocking intervention, which may be relevant for certain feed-administered compounds intended to prevent new infections rather than clear existing ones.

$$\begin{cases} \dot{S}_1 &= \Lambda_1 - m_1 S_1 - (1-\kappa)\beta_1 S_1 P, \\ \dot{L}_1 &= (1-\kappa)\beta_1 e^{-\eta_1\tau_1} S_1^{\tau_1} P^{\tau_1} - (m_1+\zeta_1)L_1, \\ \dot{I}_1 &= \zeta_1 e^{-\eta_2\tau_2} L_1^{\tau_2} - m_1 I_1, \\ \dot{S}_2 &= \Lambda_2 - m_2 S_2 - (1-\kappa)\beta_2 S_2 P, \\ \dot{L}_2 &= (1-\kappa)\beta_2 e^{-\eta_3\tau_3} S_2^{\tau_3} P^{\tau_3} - (m_2+\zeta_2)L_2, \\ \dot{I}_2 &= \zeta_2 e^{-\eta_4\tau_4} L_2^{\tau_4} - m_2 I_2, \\ \dot{P} &= e^{-\eta_5\tau_5}\left[k_1 I_1^{\tau_5} + k_2 I_2^{\tau_5}\right] - mP. \end{cases} \tag{5.2}$$

According to the reproduction number $\mathscr{R}_0^d$ previously discussed, the basic reproduction number for model (5.2) is given by the following:

$$\mathscr{R}_0^{\text{treatment}}(\kappa) = (1-\kappa)\mathscr{R}_0^d \leq \mathscr{R}_0^d.$$

Suppose that $\mathscr{R}_0^d > 1$, and that our objective is to impose $\mathscr{R}_0^{\text{treatment}}(\kappa) \leq 1$ and then the stability of the infection-free equilibrium point $\mathscr{E}_0^d$. The critical treatment efficacy κ^{cr} is given by the following:

$$\mathscr{R}_0^{\text{treatment}}(\kappa^{\text{cr}}) \quad = 1 \Longrightarrow \kappa^{\text{cr}} = 1 - \frac{1}{\mathscr{R}_0^d}.$$

Then, we obtain the following:

$$\mathscr{R}_0^{\text{treatment}}(\kappa) \quad \leq 1 \text{ for all } \kappa^{\text{cr}} \leq \kappa \leq 1;$$

thus, $\mathscr{E}_0$ is globally asymptotically stable. By choosing $\beta_1 = 0.005$ and $\beta_2 = 0.008$, we get $\kappa^{\text{cr}} = 0.8094$. Therefore,

(i) if $0.8094 \leq \kappa \leq 1$, then $\mathscr{R}_0^{\text{treatment}}(\kappa) \leq 1$, and $\mathscr{E}_0^d$ is globally asymptotically stable;
(ii) if $0 \leq \kappa < 0.8094$, then $\mathscr{R}_0^{\text{treatment}}(\kappa) > 1$, $\mathscr{E}_0^d$ becomes unstable, and the endemic equilibrium point is globally asymptotically stable.

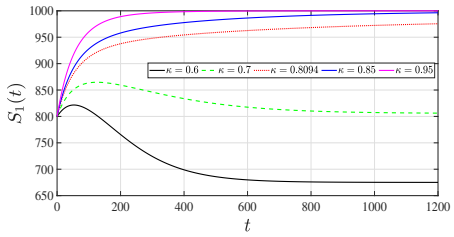

(a) Uninfected bees from colony 1.

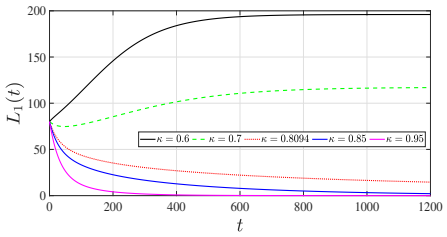

(b) Latent infected bees from colony 1.

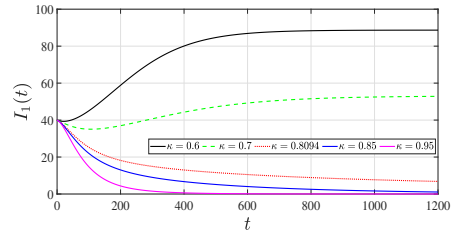

(c) Active infected bees from colony 1.

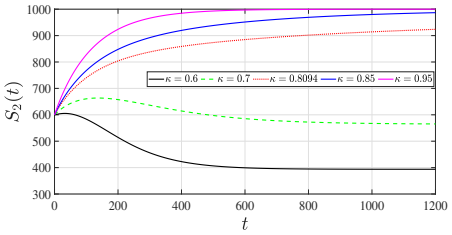

(d) Uninfected bees from colony 2.

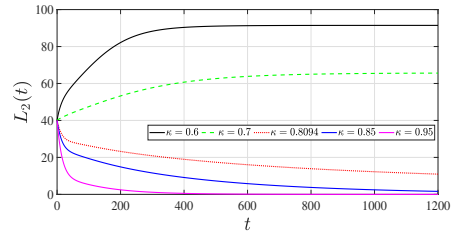

(e) Latent infected bees from colony 2.

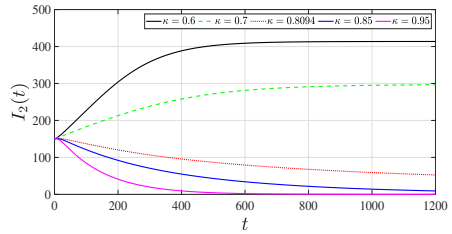

(f) Active infected bees from colony 2.

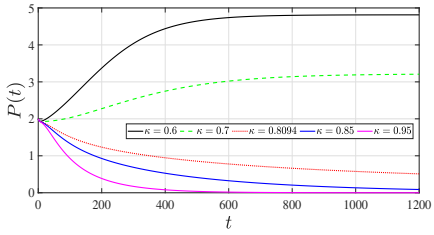

(g) Virus.

Figure 5. The solutions of system (2.1) for different treatment effectiveness rates, κ.

Table 4. The variation of $\mathscr{R}_0^{\text{treatment}}(\kappa)$ with respect to the treatment efficacy κ.

κ	0.6	0.7	0.8094	0.85	0.95
$R_0^{\text{treatment}}(\kappa)$	2.099	1.5742	1	0.7871	0.2624

Figure 5 and Table 4 illustrate the impact of the antiviral treatment efficacy, denoted by κ, on the basic reproduction number under treatment, $\mathscr{R}_0^{\text{treatment}}(\kappa)$, and on the population dynamics of the dual Nosema infection model.

The results demonstrate a clear inverse relationship between the treatment efficacy and the reproduction number. Specifically, as the value of κ increases from 0.6 to 0.95, the corresponding $\mathscr{R}_0^{\text{treatment}}(\kappa)$ decreases from 2.099 to 0.2624, as shown in Table 4. The critical drug efficacy value $\kappa_{\text{cr}} = 0.8094$ marks the threshold at which $\mathscr{R}_0^{\text{treatment}}(\kappa) = 1$. For $\kappa \geq \kappa_{\text{cr}}$, the infection-free equilibrium E_0^d becomes globally asymptotically stable, thus ensuring the elimination of the disease. The time-series plots in Figure 5 further support this analytical result. Increasing κ enhances the populations of uninfected bees in both colonies while simultaneously reducing the sizes of the latent and actively infected classes, as well as the concentration of the environmental pathogen load $P(t)$. When κ is low (e.g., $\kappa = 0.6$), the system settles around an endemic state characterized by a persistent infection. However, as κ approaches or exceeds the threshold value κ_{cr}, the trajectories of the infected compartments sharply decline, and the healthy bee populations recover toward their initial equilibrium levels.

Biologically, these results emphasize the significant role of treatment efficacy in controlling Nosema infections. A partial treatment or low drug efficacy may only mitigate symptoms without eradicating the disease, while sufficiently high efficacy levels can drive the basic reproduction number below unity, thus leading to disease extinction. Moreover, the continuous decline of $\mathscr{R}_0^{\text{treatment}}(\kappa)$ with increasing κ reflects the nonlinear yet predictable benefit of treatment intensification. Overall, Figure 5 and Table 4 confirm that antiviral treatments capable of achieving an efficacy $\kappa \geq 0.8094$ are necessary to stabilize the infection-free equilibrium and maintain the colony health. These findings provide quantitative guidance to design therapeutic and management strategies aimed at reducing pathogen transmission and sustaining the vitality of honeybee colonies.

5.4. Influence of time delays on the dynamics

In this subsection, we investigate the effect of distributed time delays on the progression and control of the dual Nosema infection within the honeybee colonies. Time delays represent biologically realistic processes such as the incubation period of the parasite, the latency between infection and spore shedding, and the maturation time of the environmental spores. By varying the delay parameters, we analyze how these temporal factors influence the stability of both the disease-free and endemic equilibria, as well as the basic reproduction number $\mathscr{R}_0^d$. Numerical simulations are employed to illustrate the dynamic outcomes under different delay scenarios, thereby highlighting conditions under which prolonged delays may hinder parasite transmission and promote infection eradication.

Among the various time-delay parameters that affect the system dynamics, the basic reproduction number $\mathscr{R}_0^d$ exhibits the highest sensitivity to changes in the delay parameter τ_5, which represents the maturation period of newly released pathogens. Owing to this pronounced influence, our analysis focuses on examining the impact of τ_5 on the overall system behavior. Using the transmission

coefficients $\beta_1 = 0.02$ and $\beta_2 = 0.03$, together with the remaining parameter values provided in Table 3, we fix $\tau_1 = \tau_2 = \tau_3 = \tau_4 = 0.1$ and vary τ_5 to investigate its effect on the stability of the disease-free equilibrium point $\mathscr{E}_0^d$. Since τ_5 explicitly appears in the analytical expression of $\mathscr{R}_0^d$, any modification of this delay directly influences the stability properties of $\mathscr{E}_0^d$. Numerical results reveal that increasing τ_5 generally leads to a decrease in $\mathscr{R}_0^d$, thus enhancing the likelihood of disease extinction and promoting system stability. To identify the critical threshold of τ_5 that guarantees the global asymptotic stability of the infection-free state, we express the basic reproduction number as a function of τ_5 as follows:

$$\mathscr{R}_0^d(\tau_5) \quad = e^{-\eta_5\tau_5}\left(\frac{\zeta_1 k_1\beta_1\Lambda_1}{mm_1^2(m_1+\zeta_1)}e^{-\eta_1\tau_1-\eta_2\tau_2}+\frac{\zeta_2 k_2\beta_2\Lambda_2}{mm_2^2(m_2+\zeta_2)}e^{-\eta_3\tau_3-\eta_4\tau_4}\right).$$

To impose that $\mathscr{R}_0^d(\tau_5) \leq 1$, we calculate the critical threshold of τ_5 as follows:

$$\tau_5^{cr} \quad = \max\left\{0, \frac{1}{\eta_5}\ln\left(\frac{\zeta_1 k_1\beta_1\Lambda_1}{mm_1^2(m_1+\zeta_1)}e^{-\eta_1\tau_1-\eta_2\tau_2}+\frac{\zeta_2 k_2\beta_2\Lambda_2}{mm_2^2(m_2+\zeta_2)}e^{-\eta_3\tau_3-\eta_4\tau_4}\right)\right\},$$

which is approximated by $\tau_5^{cr} \simeq 3.0989$ for $\beta_1 = 0.02$ and $\beta_2 = 0.03$. The following follows:

- If $\tau_5^{cr} \geq 3.0989$, then $\mathscr{R}_0^d(\tau_5) \leq 1$, thus ensuring the global stability of the infection-free equilibrium point $\mathscr{E}_0^d$;
- However, if $\tau_5^{cr} < 3.0989$, then $\mathscr{R}_0^d(\tau_5) > 1$, and in this case, the endemic equilibrium point becomes globally attractive.

Table 5 and Figure 6 summarize the influence of the maturation delay parameter τ_5 on the basic reproduction number $\mathscr{R}_0^d(\tau_5)$ and the overall disease dynamics. The results clearly show that $\mathscr{R}_0^d(\tau_5)$ monotonically decreases as the delay τ_5 increases. Specifically, as indicated in Table 5, $\mathscr{R}_0^d(\tau_5)$ declines from 1.6469 at $\tau_5 = 2.6$ to 0.4061 at $\tau_5 = 4.0$. The critical delay threshold was found to be $\tau_5^{\text{cr}} \approx 3.0989$, at which $\mathscr{R}_0^d(\tau_5) = 1$. This value represents the boundary between disease persistence and eradication: when $\tau_5 \geq \tau_5^{\text{cr}}$, the infection-free equilibrium $\mathscr{E}_0^d$ is globally asymptotically stable, whereas shorter maturation periods ($\tau_5 < \tau_5^{\text{cr}}$) allow $\mathscr{R}_0^d > 1$, thus leading to an endemic steady state. The numerical simulations depicted in Figure 6 further confirm these analytical results. As τ_5 increases, the populations of uninfected bees in both colonies steadily grow, while the numbers of latently and actively infected bees, as well as the viral concentration $P(t)$, significantly decline. This demonstrates that extending the maturation delay of newly released spores reduces the effective rate of secondary infections, thereby slowing disease transmission and promoting recovery of the healthy population.

Biologically, these findings highlight the critical role of pathogen maturation time in shaping the infection outcomes. Longer maturation periods hinder the pathogen's ability to rapidly propagate through the host population, functioning similarly to a natural control mechanism or therapeutic delay. Consequently, increasing τ_5 can be interpreted as analogous to enhancing the treatment efficacy, since both strategies effectively reduce $\mathscr{R}_0^d$ below unity and stabilize the disease-free equilibrium. In summary, Figure 6 and Table 5 demonstrate that incorporating biologically realistic time delays, particularly the maturation delay τ_5, not only alters the qualitative behavior of the system but also provides valuable insight into potential control strategies. By identifying τ_5^{cr} as a threshold for global stability, the model suggests that mechanisms which prolong parasite development or spore maturation could serve as effective means to curb the infection spread and sustain the colony health.

Table 5. Effect of the time delay τ_5 on $\mathscr{R}_0^d(\tau_5)$.

τ_5	2.6	2.8	3.0989	3.5	4
$R_0^d(\tau_5)$	1.6469	1.3484	1	0.6696	0.4061

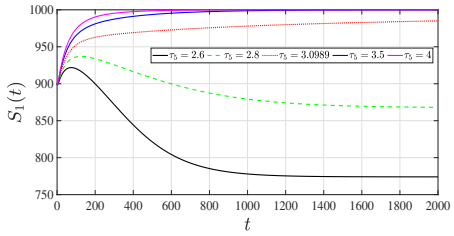

(a) Uninfected bees from colony 1.

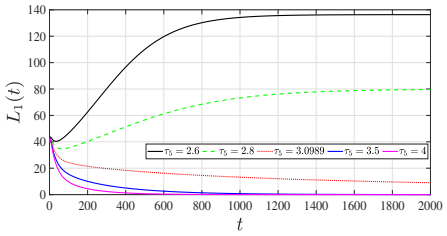

(b) Latent infected bees from colony 1.

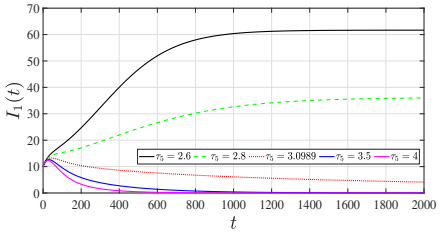

(c) Active infected bees from colony 1.

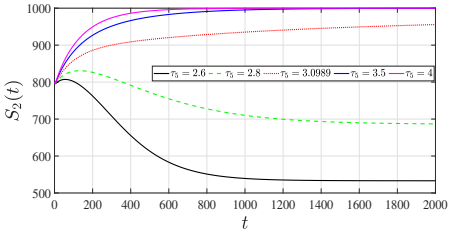

(d) Uninfected bees from colony 2.

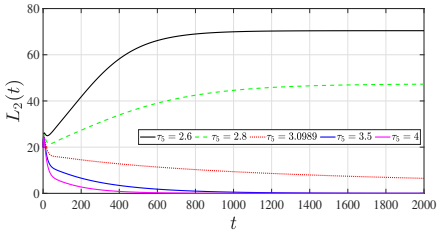

(e) Latent infected bees from colony 2.

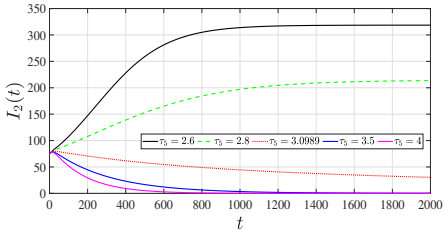

(f) Active infected bees from colony 2.

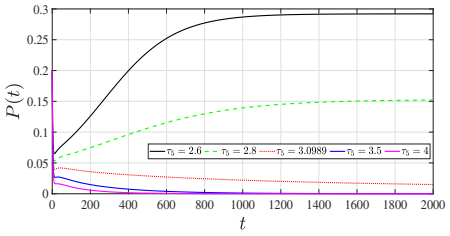

(g) Virus.

Figure 6. The solutions of system (2.1) for several time delays τ_5.

6. Conclusions

This study developed a detailed mathematical model to investigate the dynamics of dual Nosema infections in two interacting honeybee colonies, thereby incorporating biologically realistic distributed

delays and potential treatment effects. The model successfully captures key features of Nosema disease transmission, latency, infection progression, and environmental contamination shared between colonies. The analytical results established conditions for disease eradication or persistence in terms of the basic reproduction number ($\mathscr{R}_0^d$), with a rigorous treatment of stability using Lyapunov methods. The inclusion of distributed delays enhanced the biological relevance of the model by accounting for the incubation and maturation periods, which were shown to significantly influence the disease outcomes and control strategies. Numerical simulations and sensitivity analyses further highlighted the critical parameters which drive the infection dynamics, such as transmission rates, parasite shedding, and natural mortality, while also demonstrating the potential efficacy thresholds for antiviral treatments to achieve disease control.

Despite these strengths, the model has several limitations. The assumptions of constant parameter values and homogeneous mixing may oversimplify the complex behaviors and spatial heterogeneity present in real honeybee populations. Moreover, the model solely focuses on Nosema infections without explicitly integrating other co-stressors such as Varroa mites, pesticides, or nutritional factors that also critically impact the colony health. The treatment component was modeled in a generalized manner without detailed pharmacokinetics or resistance dynamics. Additionally, environmental factors such as seasonal fluctuations and climatic variability, which are known to affect Nosema prevalence and bee behavior, were not explicitly included here but could substantially alter the system's dynamics.

Future research directions include extending this framework to incorporate multi-stressor interactions and environmental seasonality, which would provide a more comprehensive understanding of honeybee colony health under realistic conditions. Spatially explicit models could better capture colony movement and localized transmission better. Integrating detailed treatment protocols and resistance development would enhance the applicability for management strategies. Experimental validation with empirical data on Nosema infection rates, latency periods, and treatment outcomes in field colonies would be invaluable to refine and calibrate the model's parameters. Finally, exploring optimal control strategies and economic assessments of intervention measures could directly inform apicultural practices and policies aimed at sustaining honeybee populations amid rising disease challenges. Overall, this work lays a strong theoretical foundation for future multidisciplinary studies on honeybee disease ecology and management.

Author contributions

All authors make equal contributions to the research work. All authors have read and agreed to the published version of the manuscript.

Use of Generative-AI tools declaration

The authors declare they have not used Artificial Intelligence (AI) tools in the creation of this article.

Acknowledgments

This work was funded by the University of Jeddah, Jeddah, Saudi Arabia, under grant No. (UJ-25-DR-20823). Therefore, the authors thank the University of Jeddah for its technical and financial

support. The authors would also like to thank the anonymous referees for many constructive suggestions, which helped to improve the presentation of the paper.

Funding

This work was funded by the University of Jeddah, Jeddah, Saudi Arabia under grant No. (UJ-25-DR-20823).

Conflict of interest

All the authors declare no conflicts of interest.

References

1. M. Higes, R. Martín, A. Meana, Nosema ceranae, a new microsporidian parasite in honeybees in Europe, *J. Invertebr. Pathol.*, **92** (2006), 93–95. https://doi.org/10.1016/j.jip.2006.02.005
2. Y. P. Chen, R. Siede, Honey bee viruses, *Adv. Virus Res.*, **70** (2007), 33–80. https://doi.org/10.1016/S0065-3527(07)70002-7
3. Y. Chen, J. D. Evans, I. B. Smith, J. S. Pettis, Nosema ceranae is a long-present and wide-spread microsporidian infection of the European honey bee (Apis mellifera) in the United States, *J. Invertebr. Pathol.*, **97** (2008), 186–188. https://doi.org/10.1016/j.jip.2007.07.010
4. J. Chen, K. Messan, M. R. Messan, G. D. Hoffman, D. Bai, Y. Kang, How to model honeybee population dynamics: Stage structure and seasonality, *arXiv Preprint*, 2020. https://doi.org/10.48550/arXiv.2003.09796
5. J. Chen, J. Rincon, G. D. Hoffman, J. Fewell, J. Harrison, Y. Kang, Impacts of seasonality and parasitism on honey bee population dynamics, *J Math. Biol.*, **87** (2023), 19. https://doi.org/10.1007/s00285-023-01952-2
6. I. Fries, Nosema apis—a parasite in the honey bee colony, *Bee World*, **74** (1993), 5–19. https://doi.org/10.1080/0005772X.1993.11099149
7. C. Mayack, D. Naug, Energetic stress in the honeybee Apis mellifera from Nosema ceranae infection, *J. Invertebr. Pathol.*, **100** (2009), 185–188. https://doi.org/10.1016/j.jip.2008.12.001
8. S. J. Martin, A. C. Highfield, L. Brettell, E. M. Villalobos, G. E. Budge, M. Powell, et al., Global honey bee viral landscape altered by a parasitic mite, *Science*, **336** (2012), 1304–1306. https://doi.org/10.1126/science.1220941
9. M. Goblirsch, Z. Y. Huang, M. Spivak, Physiological and behavioral changes in honey bees (Apis mellifera) induced by Nosema ceranae infection, *PLoS One*, **8** (2013), e58165. https://doi.org/10.1371/journal.pone.0058165
10. M. Goblirsch, Nosema ceranae disease of the honey bee (Apis mellifera), *Apidologie*, **49** (2018), 131–150. https://doi.org/10.1007/s13592-017-0535-1

11. L. Paris, H. El Alaoui, F. Delbac, M. Diogon, Effects of the gut parasite Nosema ceranae on honey bee physiology and behavior, *Curr. Opin. Insect Sci.*, **26** (2018), 149–154. https://doi.org/10.1016/j.cois.2018.02.017
12. D. S. Khoury, M. R. Myerscough, A. B. Barron, A quantitative model of honey bee colony population dynamics, *PloS One*, **6** (2011), e18491. https://doi.org/10.1371/journal.pone.0018491
13. D. S. Khoury, A. B. Barron, M. R. Myerscough, Modelling food and population dynamics in honey bee colonies, *PloS One*, **8** (2013), e59084. https://doi.org/10.1371/journal.pone.0059084
14. M. I. Betti, L. M. Wahl, M. Zamir, Effects of infection on honey bee population dynamics: A model, *PLOS One*, **9** (2014), 1–12. https://doi.org/10.1371/journal.pone.0110237
15. M. Betti, L. Wahl, M. Zamir, Age structure is critical to the population dynamics and survival of honeybee colonies, *Roy. Soc. Open Sci.*, **3** (2016), 160444. https://doi.org/10.1098/rsos.160444
16. A. Dénes, M. A. Ibrahim, Global dynamics of a mathematical model for a honeybee colony infested by virus-carrying Varroa mites, *J. Appl. Math. Comput.*, **61** (2019), 349–371. https://doi.org/10.1007/s12190-019-01250-5
17. M. El Hajji, F. A. S. Alzahrani, M. H. Alharbi, Mathematical analysis for Honeybee dynamics under the influence of seasonality, *Mathematics*, **12** (2024), 3496. https://doi.org/10.3390/math12223496
18. M. El Hajji, F. A. S. Alzahrani, R. Mdimagh, Impact of infection on Honeybee population dynamics in a seasonal environment, *Int. J. Anal. Appl.*, **22** (2024), 75. https://doi.org/10.28924/2291-8639-22-2024-75
19. J. K. Hale, A. S. Somolinos, Competition for a fluctuating nutrient, *J. Math. Biol.*, **18** (1983), 255–280. https://doi.org/10.1007/BF00276091
20. A. Korobeinikov, Global properties of basic virus dynamics models, *B. Math. Biol.*, **66** (2004), 879–883. https://doi.org/10.1016/j.bulm.2004.02.001
21. S. K. Sasmal, I. Ghosh, A. Huppert, J. Chattopadhyay, Modeling the spread of Zika virus in a stage-structured population: Effect of sexual transmission, *B. Math. Biol.*, **80** (2016), 3038–3067. https://doi.org/10.1007/s11538-018-0510-7
22. N. Chitnis, J. M. Hyman, J. M. Cushing, Determining important parameters in the spread of malaria through the sensitivity analysis of a mathematical model, *B. Math. Biol.*, **70** (2008), 1272–1296. https://doi.org/10.1007/s11538-008-9299-0
23. J. K. Hale, S. M. V. Lunel, *Introduction to functional differential equations*, New York: Springer-Verlag, 1993. https://doi.org/10.1007/978-1-4612-4342-7
24. P. V. den Driessche, J. Watmough, Reproduction numbers and sub-threshold endemic equilibria for compartmental models of disease transmission, *Math. Biosci.*, **180** (2002), 29–48. https://doi.org/10.1016/S0025-5564(02)00108-6
25. J. P. LaSalle, *The stability of dynamical systems*, SIAM: Philadelphia, 1976.
26. H. Khalil, *Nonlinear systems*, 2Eds, Prentice Hall, 1996.
27. H. H. Almuashi, M. El Hajji, Global dynamics of a dual-target HIV model with time delays and treatment implications, *Mathematics*, **14** (2026). https://doi.org/10.3390/math14010006

28. N. A. Almuallem, M. El Hajji, Global dynamics of a multi-population water pollutant model with distributed delays, *Mathematics*, **14** (2026). https://doi.org/10.3390/math14010020

29. S. Marino, I. B. Hogue, I. B. Ray, D. E. Kirschner, A methodology for performing global uncertainty and sensitivity analysis in systems biology, *J. Theor. Biol.*, **254** (2008), 178–196. https://doi.org/10.1016/j.jtbi.2008.04.011

AIMS Press